Phenoxy-Amidine Ligands: Toward Lactic Acid-Tolerant Catalysts for Lactide Ring-Opening Polymerization

Valentin Vaillant-Coindard, Benjamin Théron, Gaël Printz, Florian Chotard, Cédric Balan, Yoann Rousselin, Philippe Richard, Iogann Tolbatov, Paul Fleurat-Lessard, Ewen Bodio, et al.

Phenoxy-Amidine Ligands: Towards Lactic Acid-Tolerant Catalysts for Lactide ROP

Valentin Vaillant-Coindard,[†+] Benjamin Théron,[†+] Gaël Printz,[§] Florian Chotard,[†] Cédric Balan,[†] Yoann Rousselin,[†] Philippe Richard,[†] Iogann Tolbatov,[†] Paul Fleurat-Lessard,[†] Ewen Bodio,[†] Raluca Malacea-Kabbara,[†]* Jérôme Bayardon,[†] Samuel Dagorne[§]* and Pierre Le Gendre[†]*

[†]Institut de Chimie Moléculaire de l'Université de Bourgogne (ICMUB, UMR-CNRS 6302), Université Bourgogne Franche-Comté

[§]Institut de Chimie de Strasbourg (UMR-CNRS 7177), Université de Strasbourg

[+]These authors contributed equally

ABSTRACT: The replacement of the imine functionality in the ubiquitous phenoxy-imine (FI) ligands by a more robust and donor *N*,*N*,*N*'-trisubstituted amidine function was examined and gave rise to the synthesis of five new phenoxy-amidine (FA) ligands (**L1**-**L5**). The solid-state structure of four proligands has been determined by X-ray diffraction analysis and showed that the amidine moiety is in *trans*-configuration. The reaction of the phenol-amidine proligands with $AlMe_3$ afforded mononuclear (**L1**-**L5**)$AlMe_2$ (**1a**-**5a**). A similar alkane elimination route was used from $ZnEt_2$ and led to dinuclear [(**L1**-**L5**)$ZnEt]_2$ complexes (**1b**-**5b**) or to homoleptic (**L2**/**L4**)$_2$Zn complexes (**2b'**, **4b'**) depending on the metal:ligand ratio used. The structure of these complexes has been determined by NMR spectroscopy (^{1}H, ^{13}C, HMBC, HSQC, DOSY, and NOESY experiments) and X-Ray diffraction study for seven of them. The crystal structure of the Al complexes showed FA ligands coordinated in a chelate fashion *via* the O atom of the aryloxy group and the imino-*N* atom indicating that the amidine function has undergone *trans*-*cis* isomerization upon coordination. A similar chelating coordination mode was observed for the FA ligands with Zn metal ions. These complexes were used as initiators for the ring-opening polymerization (ROP) of *rac*-lactide. FA-Zn complexes gave the best performance affording polylactic acid (PLA) with narrow molecular weight distribution and heterotactic bias (Pr up to 0.75). Remarkably, some of these complexes were able to tolerate the presence of a large amount of lactic acid to the point of using it as a co-initiator during the polymerization reaction.

INTRODUCTION

Phenoxy-imines (FI) ligands represent one of the most useful class of ligands for catalysis (Fig. 1).[1,2,3] Their ease of access and structural modularity allowed the synthesis of a great variety of metal complexes that enables thorough screening processes and the identification of highly performant systems for many different catalytic transformations. However, one drawback of this class of ligands is the sensitivity of imines that can undergo various reactions (hydrolysis, reduction,[4] alkylation,[5] …) and, consequently, cause the degradation of the catalyst. With this in mind, we considered a related class of ligands in which the imine function is replaced by a trisubstituted amidine giving rise to phenoxy-amidine (FA) ligands. The additional NR_2 group in the amidine moiety should bring steric protection and electronic density to the otherwise exposed electrophilic imine carbon atom and, hence, makes ligands less sensitive to reducing or nucleophilic reagents as compared to FI. We also anticipated that the π-donor ability of the amidine moiety should provide better stabilization to electron deficient metal ions. Based on this approach, we recently reported a first generation of phenoxy-amidine ligand (1FA) in which the amidine is *N*-linked to the phenoxy moiety through a methylene spacer (Fig. 1).[6] However, a disadvantage of the introduction of a methylene linker is that it precludes conjugation and may limit the potential of FA ligands. Indeed, it has been shown that the π-conjugated character of the FI ligands confers some "electronic flexibility" to the chelated metal active species, and this contributes to the good catalytic performance.[1a,7] With this in mind, we targeted a second generation of FA ligands (2FA) structurally closer to FI, where the *N*,*N*,*N'*-trisubstituted amidine is directly C-linked and thus conjugated with the phenoxy moiety (Fig. 1).

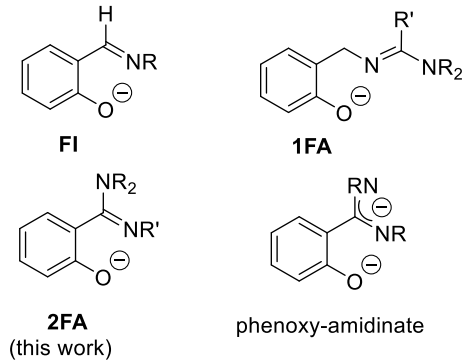

Figure 1. Phenoxy-imines (FI), phenoxy-amidines (FA) and phenoxy-amidinate derivatives.

It should be mentioned that in previous studies, Carpentier and Kirillov described the coordination chemistry of phenoxy-amidinates (Fig. 1) and showed that these dianionic ligands are more likely to bridge two metals than to chelate one.[8] On the other hand, and this was rather encouraging for our purposes, they also showed that the protonated form of the ligand (i.e. phenoxy-amidine) can form chelate complexes with Zr(IV). Herein, we report the synthesis of FA ligands of 2nd generation as well as their coordination chemistry with Zn(II) and Al(III) metal ions. We have chosen to evaluate the performance of FA ligands for the ring-opening polymerization (ROP) of *rac*-lactide. One of the challenges in this field concerns the development of robust and efficient catalysts to replace tin(II) octoate, currently used in industry. Great efforts have been made, and very active systems with different metals have been described.[9] However, most of them only work with recrystallized and sublimed lactide monomer, free of any trace of lactic acid and water, unlike the lactide used in the industry. Recently, Jones reported FI-Zn complexes capable of promoting ROP of LA under bulk conditions from "not rigorously purified" monomers.[2g,2h] Guanidine Zn complexes described by Herres-Pawlis also showed up as effective despite the use of technical grade lactide.[10] We hypothesized that FA ligands with a robust and electron-donating amidine functionality could also be good candidates to access catalysts capable of withstanding a certain level of protic impurities, a crucial point for industrial applications.

RESULTS AND DISCUSSION

Synthesis of ligands and complexes. The synthesis of the phenol-amidine proligands **L1H-L5H** is outlined in Scheme 1 and was performed in one-pot three-step reaction either from 2-benzyloxybenzamide derivatives (**L1H**, **L2H**) or from 2-methoxybenzamide derivatives (**L3H-L5H**). Chlorination of these compounds using oxalyl chloride afforded the corresponding chlorobenziminium chloride ion intermediates, which were further reacted with the appropriate amine in the presence of triethylamine.[11] Deprotection of the phenol group from their respective benzyl or methyl ether furnished the phenol-amidine proligands in 33-62% yields. **L1H** and **L2H** could also be synthesized from 2-methoxybenzamide derivatives but with lower yields due to their partial solubility. in water, which hampered product isolation during aqueous treatment at the deprotection step. Suitable crystals for X-Ray diffraction studies were obtained for **L2H-L5H** proligands (Fig. 2). In the solid state, the amidine. group of each proligand adopt the same *trans* configuration, sp^2 character for the nitrogen atom N2 ($\Sigma\alpha_{N2} \approx 360°$) and coplanar alignment of the NR_2 group with the amidine plane ($\theta \approx 0°$). Another common feature of the four proligand structures is the almost orthogonal orientation of the phenol ring with respect to the amidine plane ($79° < |\psi| < 109°$). In addition, crystal packing shows intermolecular H-bonds between the phenolic protons of the proligand and the amidine-N atoms of the neighboring molecule giving rise to polymeric chains. Consequently, rather small Δ_{CN} parameters (Δ_{CN} = d(C-N) - d(C=N)) ranging from 0.027 Å to 0.066 Å are observed. This reflects significant delocalization along the N=C–N moiety which is less pronounced in **L2H**. The ^{1}H NMR spectra of **L1H-L5H** show only one isomer in solution, which we assume to be *trans* isomer based on solid state structures and NOESY experiments (*vide infra*). The other noticeable point in these spectra is the broadening of the NR_2 signal(s), which can be attributed to a partial restricted rotation around the amidine C-NR_2 bond.

Scheme 1. Synthesis of the phenol-amidine proligands

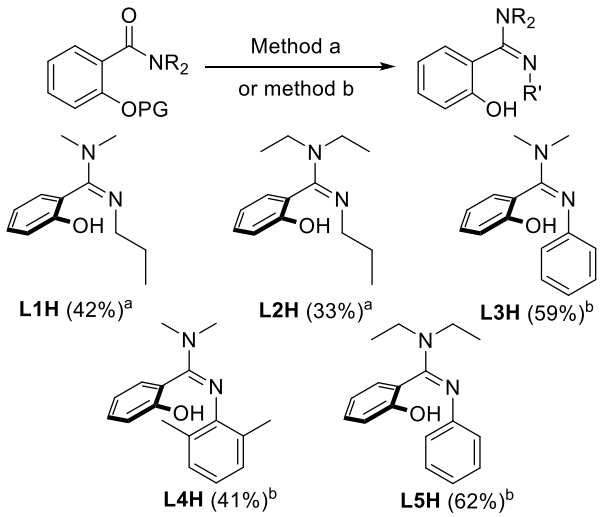

Method a (PG = Bn): *i)* $(COCl)_2$, toluene, 60°C, 15 h; *ii)* *n*-$PrNH_2$ (5 equiv.), DCM, r.t., 15 h; *iii)* Pd/C 10%, H_2 (10 bar), ethanol, r.t. 15 h / **method b** (PG = Me): *i)* $(COCl)_2$, toluene, 60°C, 2 d; *ii)* $ArNH_2$ (1.2 equiv.), NEt_3 (5 equiv.), DCM, r.t., 15 h; *iii)* BBr_3, DCM, r.t., 15 h then $NaOH_{aq}$

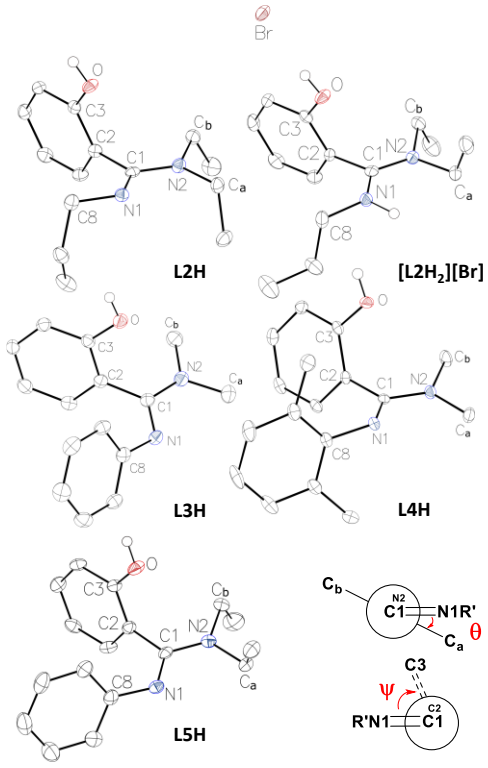

Figure 2. ORTEP views of **L2H-L5H** and **[L2H$_2$][Br]** (Hydrogen atoms, except hydroxy and amidinium protons, as well as the second independent molecule for **L5H** are omitted for clarity) and definition of the torsion angles θ (N1C1N2C_a) and ψ (N1C1C2C3). Selected distances (Å) and angles (°) of: **L2H** C1–N1 1.294(2), C1–N2 1.360(2), $\Sigma\alpha_{N2}$ 359.9(4), θ 0.1(2), ψ 79.6(2); **[L2H$_2$][Br]** C1–N1 1.329(3), C1–N2 1.315(3), $\Sigma\alpha_{N2}$ 359.9, θ 0.9(4), ψ 85.3(3); **L3H** C1–N1 1.316(2), C1–N2 1.343(2), $\Sigma\alpha_{N2}$ 359.9(6), θ 7.3(3), ψ -108.7(2); **L4H** C1–N1 1.300(1), C1–N2 1.355(1), $\Sigma\alpha_{N2}$ 359.7(3), θ 4.6(2), ψ 105.7(1); **L5H** C1–N1 1.305(6), C1–N2 1.345(6), $\Sigma\alpha_{N2}$ 359.9(1.2), θ -4.4(6), ψ 104.8(5). Thermal ellipsoids are drawn at 50% probability level.

VT NMR experiments were conducted on **L3H** and allow to determine a rotational barrier of 57.3(2) kJ mol^{-1} from Eyring equation (Fig. S16, SI). No signal corresponding to the presence of the other phenol-(*cis*-amidine) isomer was observed down to 228 K. The basic character of the phenoxy-amidine ligands was evidenced with **L2H**, which was converted into phenol-amidinium bromide **[L2H$_2$][Br]** by addition of aqueous bromohydric acid. The solid-state molecular structure of **[L2H$_2$][Br]** shows a geometry and *trans* configuration similar to that of **L2H** with smaller Δ_{CN} value (Δ_{CN} = 0.013) indicating more pronounced delocalization within the amidinium moiety. The ^{1}H NMR spectrum of **[L2H$_2$][Br]** shows two sets of signals for the two ethyl groups due to more restricted rotation around the C-NEt$_2$ bond and diastereotopic splitting of the signals of the methylene protons, likely indicative of axial chirality due to restricted rotation between the hydroxyaryl and the amidinium moieties. NOESY NMR experiment conducted on **[L2H$_2$][Br]** shows an interaction between the amidinium (NH) proton at 9.25 ppm and one methylene proton of an ethyl group located at 3.91 ppm suggesting that the *trans* configuration of the amidinium salt observed in the solid-state is preserved in solution (Fig. S33, SI).

We then explored the coordination chemistry of these proligands with Al(III). The reaction of equimolar amounts of **L1H-L5H** and AlMe$_3$ in THF or dichloromethane at room temperature afforded the corresponding aluminum complexes **1a-5a** in 37 to 72% yields (Scheme 2). Single crystals of **2a-5a** complexes were obtained and analyzed by X-Ray diffraction (Fig. 3). All four complexes present a pseudo-tetrahedral geometry around the Al atom, with the FA ligands that bind to aluminum in κ^2-fashion and two residual methyl ligands. Thus, if (as seems likely) the proligands exist in solution in *trans* form, it means that amidine has undergone isomerization during the reaction with AlMe$_3$ (imino N-substituent R' switched from *trans* to *cis* position with respect to amino nitrogen). At this point, we should mention that amidines isomerization has been the subject of several studies and the kinetics of isomerization were found comparable to those reported for isomerization of imines.[12,13] Coordination to aluminum results in smaller Δ_{CN} values than in the proligands except in the case of **3a** (Table 1). The Al-C, Al-N and Al-O bond distances are very similar for the four complexes **2a-5a** and in the range of the bond lengths observed in the FI aluminum complexes Me$_2$Al{OC$_6$H$_4$[2-(CH=NPh)]} **I** previously reported by Lewiński and Zachara.[14]

The most striking structural difference between FA and FI complexes is the distance (D) from the Al center to the aryloxy plane, which is much higher in the former case (1.05(13) Å in **3a** and 1.277(2) in **5a** *vs* 0.275(3) Å in **I**). Consistently, the amidine and aryloxy ring are not coplanar and form a dihedral angle (ψ) between 24.1(3)° and 35.0(4)°, in absolute term. It should also be noted that the NR$_2$ moieties are tilted with respect to the amidine plane as indicated by the torsion angle (θ) which ranges between 25.6(6)° and 45.8(2)°, in absolute term.

Scheme 2. Synthesis of the FA aluminum complexes

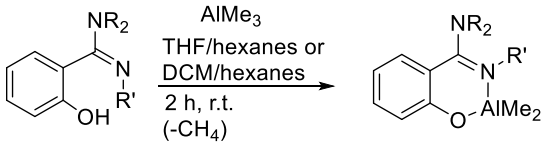

L1H-L5H

1a (R = Me, R' = Pr) 37%
2a (R = Et, R' = Pr) 72%
3a (R = Me, R' = Ph) 63%
4a (R = Me, R' = 2,6-(CH$_3$)$_2$C$_6$H$_3$) 66%
5a (R = Et, R' = Ph) 64%

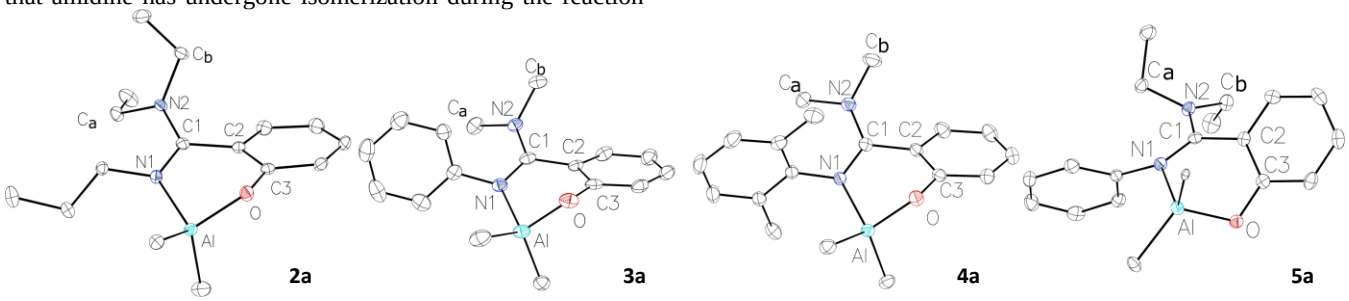

Figure 3. ORTEP views of **2a-5a** (Hydrogen atoms, molecules of solvent as well as the second independent molecules for **3a** and **4a** are omitted for clarity). Thermal ellipsoids are drawn at 50% probability level.

Table 1. Relevant bond distances (Å) and angles (°) in compounds 2a-5a.

	C1-N1	C1-N2	Al-Me	Al-O	Al-N1	D[a]	θ[b]	ψ[b]
2a	**1.315(2)**	**1.372(2)**	**1.959(2)** **1.972(2)**	**1.784(1)**	**1.946(1)**	**0.987(2)**	**-45.8(2)**	**-27.6(1)**
3a[c]	**1.325(2)**	**1.358(4)**	**1.954(2)** **1.965(5)**	**1.785(1)**	**1.951(7)**	**1.05(13)**	**-29.8(8)**	**-24.1(3)**
4a[c]	**1.321(2)**	**1.353(2)**	**1.961(2)** **1.978(2)**	**1.785(2)**	**1.958(3)**	**1.206(15)**	**-25.6(6)**	**-34.5(8)**
5a	**1.328(3)**	**1.357(3)**	**1.960(3)** **2.005(2)**	**1.798(2)**	**1.962(2)**	**1.277(2)**	**28.1(4)**	**35.0(4)**
I[d]	**1.296(3)**	**-**	**1.943(3)** **1.946(3)**	**1.772(2)**	**1.963(2)**	**0.275(3)**	**-**	**6.9(4)**

[a]: D = distance in between Al atom and the aryloxy plane [b]: defined as in Fig. 2 [c]: the values of only one of the two independent molecules are reported [d]: ref 14.

It is likely that the steric crowding between the NR_2 group and the aryloxy ring prevent the FA ligands from adopting a more coplanar orientation, thus positioning the metal out of the mean plane of the aryloxy group. As compared to the proligands, the ^{1}H NMR spectra of the aluminum complexes **1a**-**5a** show the additional signal of the $AlMe_2$ group at ca. -1 ppm and better resolved and sharper signal for the NMe_2 group (set of signals for NEt_2) consistent with the fast rotation around the amidine bond on the NMR timescale.

FA ligands were next coordinated to Zn(II) *via* an alkane elimination route similar to the one used in Al series. Thus, the phenol-amidine proligands **L1H**-**L5H** were reacted with $ZnEt_2$ in THF/hexane or DCM/hexane mixture at room temperature to yield the FA ethyl zinc dimeric complexes **1b**-**5b** in 54 to 90% yields (Scheme 3). Single crystals of **2b** and **3b** complexes were obtained and analyzed by X-Ray diffraction (Fig. 4).

Scheme 3. Synthesis of the FA zinc complexes

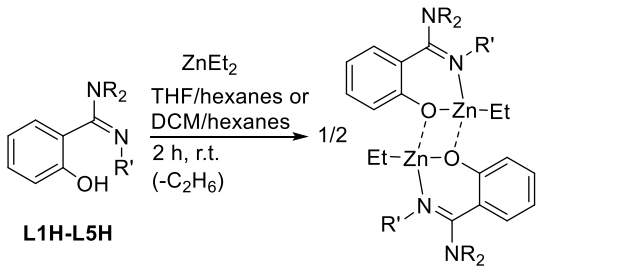

1b (R = Me, R' = Pr) 54%
2b (R = Et, R' = Pr) 90%
3b (R = Me, R' = Ph) 65%
4b (R = Me, R' = 2,6-$(CH_3)_2C_6H_3$) 85%
5b (R = Et, R' = Ph) 78%

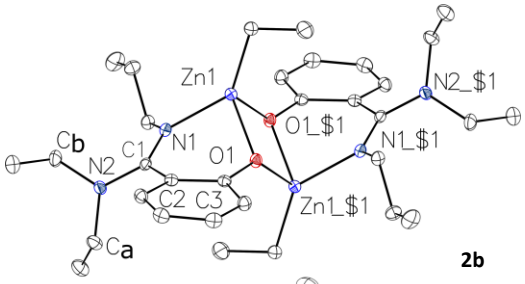

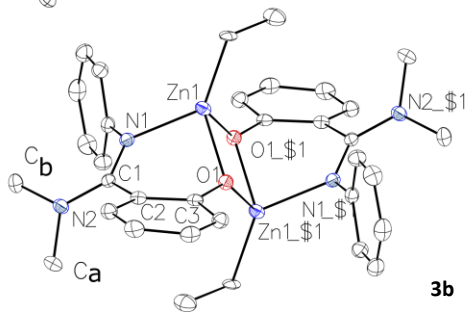

Figure 4. ORTEP view of complexes **2b** and **3b** (Hydrogen atoms, as well as the second independent molecule for **2b** are omitted for clarity. Selected distances (Å) and angles (°) of: **2b** C1–N1 1.299(2), C1–N2 1.381(1), Zn-Et 1.975(1), Zn-O 2.052(1), Zn-N1 2.030(1), D 1.296(1), θ -47.7(2), ψ -32.47(2); **3b** C1–N1 1.307(3), C1–N2 1.364(3), Zn-Et 1.984(2), Zn-O 2.024(1), Zn-N1 1.984(2), D 1.499(1), θ -21.1(3), ψ -40.7(3).Thermal ellipsoids are drawn at 50% probability level. Symmetry equivalent atoms are generated by the symmetry code $1 (-x,1-y,1-z) and $1 (1-x,1-y,1-z) for **2b** and **3b**, respectively.

2b crystalizes in the *P*-1 triclinic space group and **3b** crystalizes in the $P2_1/n$ triclinic space group, one half molecule is present in the asymmetric unit for both structures. In both complexes the Zn centers are coordinated by a FA ligand in κ*N*,κ*O* chelate fashion, one ethyl group and one bridging oxygen atom from the second FA ligand, yielding a pseudo tetrahedral geometry. Thus, like in the Al series, FA ligands have undergone *trans-cis* isomerization upon coordination with Zn(II). Both Zn complexes solid state structures show higher Δ_{CN} values than their Al counterpart and Zn-O/-N/-C bond lengths in the range of those observed in previously described FA and FI Zn complexes.[6,2g] Like in (FA)Al complexes, FA ligands adopt non planar conformation and Zn centers are sited out of the aryloxy plane. The ^{1}H NMR spectra of complexes **3b**-**5b** display expected resonance patterns consistent with the proposed structures while the ^{1}H NMR spectra of **1b** and **2b** complexes in CD_2Cl_2 show poorly resolved and broad signals partly overlapping each other and difficult to interpret. Variable-temperature ^{1}H NMR study as well as DOSY and NOESY NMR experiments were carried out on complex **2b** (Fig. S74-S75 and S108, SI). These NMR data show that complex **2b** exists in CD_2Cl_2 solution as dimers that exchange in a dynamic equilibrium on NMR time. In parallel, the use of deuterated pyridine solvent allowed the NMR characterization of **2b** in its presumed monomeric form as a pyridine adduct. One should also mention that VT NMR experiment conducted in parallel on **3b** showed no significant evolution of the ^{1}H NMR spectrum *vs* temperature (Fig. S77, SI) and DOSY NMR experiments also established the dimeric structure of **3b** in solution (Fig. S109, SI). We hypothesize that the singular NMR behavior of **2b** (and **1b**) in CD_2Cl_2 is due to the hindered motion of the propyl group giving rise to slow exchange on the NMR time scale between rotamers around the C_{Pr}-N bond on both sides of the dimeric complex. To check our hypothesis, we theoretically sampled the conformational space of complexes **2b** and **3b**. As anticipated, there exist 6 families of low lying ($\Delta E \leq$ 2 kcal/mol) conformers for **2b**, while **3b** exhibits only one stable conformation corresponding to the X-Ray structure (Fig. S112, SI).

ROP of Lactide. A variety of Zn(II) and Al(III) complexes bearing FI ligands have been reported previously as catalytically active for the polymerization of both *L*-lactide and *rac*-lactide.[2a,2c,2e,2g,15,16] The polymerization reactions are most often carried out either in dichloromethane, toluene or in the bulk at temperature ranging from r.t. to 180°C and at different catalyst loadings. With the aim to compare the polymerization performance of FA and FI complexes under similar conditions, we synthesized the new complexes **6a** and **6b** (Fig. 5) from the *N*-(*n*-propyl) FI ligand **L6H** (see S61, SI). We then tested them in parallel with complexes **1a**-**5a** and **1b**-**5b** as ROP initiators of *rac*-lactide in the presence of 1 equiv. of ^{i}PrOH as the alcohol source. The Al complexes were able to promote the ROP of unpurified *rac*-lactide (used as received) affording atactic PLAs with 66-95% conversion after 14.5 h at 90°C (Table 2). The complexes with NMe_2–substituted FA ligands gave higher activities than their NEt_2–counterparts. GPC analysis showed PLA with relatively narrow molecular weight distributions(1.23-1.43), M_n values close to the calculated ones for the complexes bearing *N*-aryl substituents on the imino-carbon (**3a**-**5a**) and lower values than expected for complexes **1a**-**2a** with *N*-propyl amidine FA ligands. Comparison with complex **6a** or with other FI Al complexes previously reported in the literature shows that FI and FA ligands give similar performance.[16]

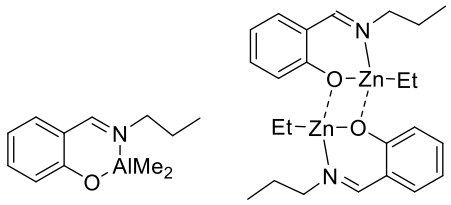

Figure 5. Al and Zn-FI complexes **6a** and **6b** synthesized for comparative purposes.

Table 2. ROP of lactide mediated by FA-Al complexes **1a**-**5a** and FI-Al complex **6a**[a,b]

Init.	Conv (%)[c]	$M_{n,\,exp}$ (Đ)[d]	$M_{n,\,theo}$[e]	P_r[f]
1a	95	8 600 (1.43)	13 700	0.52
2a	66	6 100 (1.23)	9 500	0.48
3a	93	12 000 (1.32)	13 400	0.53
4a	92	11 200 (1.33)	13 300	0.55
5a	89	13 100 (1.33)	12 800	0.55
6a	95	11 500 (1.58)[g]	13 700	0.51

[a] Polymerization conditions: [*rac*-LA]$_0$ = 1.5 M, 100 equiv. of *rac*-LA, 1 equiv of ^{i}PrOH and 1 equiv of metal catalyst, toluene, 90°C, 14.5 h. [b] Reactions performed with a batch of unpurified *rac*-LA. [c] Monomer conversion. [d] Measured by GPC in THF (30 ˚C) using PS standards and corrected by applying the appropriate correcting factor (0.58). [e] Calculated using $M_{n,theo}$ = [*rac*-LA]$_0$/[catalyst]$_0$ × M_{LA} × conversion. [f] Determined from the methine region of the HD ^{1}H NMR spectrum. [g] GPC chromatogram presents bimodal profile (Fig. S116, SI).

Expectedly, Zn complexes were found to be more reactive than their Al counterparts (Table 3). Compounds **1b** and **2b** afforded PLA with almost complete conversion after 2 h at room temperature. Complexes **3b**-**5b** bearing an aryl group on the imino-nitrogen appeared slightly less active. All catalysts yielded PLA with narrow molecular weight distributions (PDI = 1.04-1.12), however, with a better match of experimental and calculated M_n values for the *N*-aryl-substituted FA complexes **3b**-**5b**. ^{1}H NMR analysis of the PLA samples showed that the Zn complexes produced slightly heterotactic-enriched polymers with higher heteroselectivities for complexes **3b** and **4b** (P_r = 0.66 and 0.68, respectively). The kinetic of the ROP of LA was further examined with complex **2b**. The semilogarithmic plot of Ln([LA]/[LA]$_0$) against time shows a linear relationship (k_{app} = 0.02 min^{-1}) indicating first order consumption of LA (Fig. S118, SI). A linear relationship between the number-average molecular weight and the monomer conversion was also observed confirming the ability of complex **2b** to perform well controlled polymerization. In addition, MALDI-ToF analysis shows PLA chains with isopropoxy ester end-groups, with some minor transesterification reactions (Fig. S119, SI). Comparison between the performances of FA and FI Zn complexes bearing the same *N*-propyl substituent (**6b** *vs* **1b** and **2b**) suggests that the additional NR_2 fragment present in amidine has a rather limited impact on polymerization results.

However, in some polymerization trials, LA monomer stored for a few months under air and *de facto* contaminated with water and lactic acid (4 mol% according to NMR measurement) was fortuitously used, resulting in completely different trends for Zn complexes. As illustrated in Table 3, the FI-Zn complex **6b** as well as the *N*-aryl-substituted FA complexes **3b**-**5b** led to

Table 3. ROP of lactide mediated by FA-Zn complexes **1b**-**5b** and FI-Zn complex **6b**[a]

Init.	Conv (%)[b]	$M_{n,\,exp}$ (Đ)[c]	$M_{n,\,theo}$[d]	P_r[e]
1b[f]	92	10 500 (1.10)	13 300	0.59
2b[f]	93	10 400 (1.11)	13 400	0.56
3b[f]	73	9 900 (1.07)	10 500	0.66
4b[f]	80	8 500 (1.04)	11 500	0.68
5b[f]	46	6 000 (1.08)	6 600	0.62
6b[f]	93	11 100 (1.07)	13 400	0.60
1b[g]	93	7 300 (1.11)	13 400	n.d.
2b[g]	97	11 000 (1.18)	14 000	n.d.
3b[g]	0	-	-	-
4b[g]	0	-	-	-
5b[g]	0	-	-	-
6b[g]	0	-	-	-

[a] Polymerization conditions: [*rac*-LA]$_0$ = 1.5 M, 100 equiv of *rac*-LA, 1 equiv of ^{i}PrOH and 0.5 equiv of **1b**-**6b** (1 equiv of Zn), CH_2Cl_2, 20°C, 2 h. [b] Monomer conversion. [c] Measured by GPC in THF (30 ˚C) using PS standards and corrected by applying the appropriate correcting factor (0.58). [d] Calculated using $M_{n,theo}$ = [*rac*-LA]$_0$/[Zn]$_0$ × M_{LA} × conversion. [e] Determined from the methine region of the HD ^{1}H NMR spectrum. [f] Reactions performed with a batch of unpurified LA. [g] reaction performed with a batch of LA contaminated with lactic acid (4 mol%) and significant amount of water.

no polymer after 2 h, whereas complex **1b** and **2b** converted 93 and 97% of impure LA, respectively, to PLA. The unexpected ability of complexes **1b** and **2b** to promote the ROP of lactide in the presence of four-fold excess of lactic acid (vs. initiator) caught our attention. To confirm this behavior, ROP of purified LA were performed using **2b**, isopropanol and exogenous lactic acid in 1:1:1 ratio (Table 4, entry 1). PLA was obtained with 88% lactide conversion after only 40 min, with narrow polydispersity and an average molecular weight lower than predicted for the produced PLA. Reactions performed in the same conditions but only with either isopropanol or lactic acid afforded lower conversions but with a better fit between experimental and calculated M_n values (Table 4, entries 2,3). At last, polymerization did not proceed in the presence of **2b** only (Table 4, entry 4). To characterize the end groups of polymers, we performed a MALDI-ToF analysis on short PLA chains obtained by limiting the polymerization reaction time to 10 min. MALDI-ToF analysis of the PLA polymers obtained in the presence of lactic acid showed a series of main peaks at $(144{,}042)_n$ (PLA) + 90.03 (lactic acid) + 22,99 (Na^+) Da which can be ascribed to PLA chains end-capped with lactic acid and an additional sodium cation (Fig. 6). Noteworthy, two series of shorter chain polymers were also observed at $(144.042)_m$ (PLA) + 18.01 (H_2O) + 22.99 (Na^+) Da and $(144.042)_p$ (PLA) + 22,99 (Na^+) Da due to chains terminated by an OH group and to cyclic polymers. MALDI-TOF spectra of PLA obtained with higher conversion but in more diluted conditions ([*rac*-LA] = 0.5 M) and with lower ratio of monomer to initiator ([*rac*-LA]:[Zn]$_0$:[lactic acid] = 25:1:1) show mainly short chains corresponding to cyclic polymers (Fig. S120, SI). MALDI-ToF spectra of the polymers obtained in the presence of both lactic acid and isopropanol, confirmed the polymers to be either

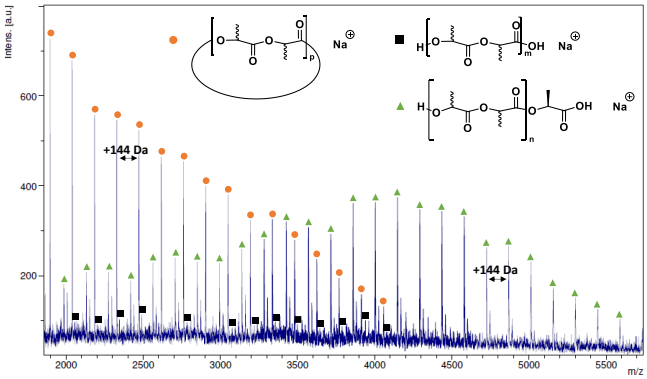

Figure 6. MALDI-TOF spectra of PLA produced using **2b** with lactic acid as initiator (20°C, 10 min, 100:1:1)

terminated by an O^{i}Pr end-group or by a lactid acid unit. Polymerization experiments were next performed to determine whether **2b** could withstand other α–hydroxy acids. Lower LA conversion (72%) and broader polydispersity (Đ = 1.83) were seen when polymerization was conducted in the presence of glycolic acid instead of isopropanol or lactic acid (Table 4, entry 6), which can be attributed to the low solubility of glycolic acid in DCM. On the other hand, the reaction conducted with glycolic acid resulted in higher heterotacticity (P_r = 0.75). The use of *rac*-mandelic acid as co-initiator led to slightly heterotactic PLA with almost complete conversion after 2 h at room temperature (Table 4, entry 7). The GPC analysis showed polymers with higher molecular weights than the values predicted and relatively narrow molecular weight distributions (Đ = 1.29). The MALDI-ToF spectra of the PLA polymers obtained using mandelic or glycolic acid as co-initiators showed similar pattern to those observed with lactic acid: a main series of peaks splitted by 144 Da which corresponds to chains terminated by α–hydroxy acid end-groups and two series of shorter chains separated by 144 Da due to OH-terminated PLAs and to cyclic polymers (Fig. S121-S122, SI). The observation of cyclic polymers, mainly with an integer number of monomers, suggests intramolecular esterification (back-biting) that can easily occur if growing polymer chains with a pendant anhydride function are formed.[17]

Given the dramatic difference of performance of the complexes (**1b**-**6b**) in the presence of lactic acid, ^{1}H NMR monitoring experiments were performed to probe their reactivity with lactic acid. The addition of one equiv. of lactic acid to CD_2Cl_2 solutions of two representative complexes (**2b** and **4b)** led in both cases to the formation of a precipitate, assumed to be Zn lactate adducts. These complexes were shown inactive in ROP of LA. Based on ^{1}H NMR data, the residual species present in solution are consistent with homoleptic complexes **2b'** [(**L2**)$_2$Zn] and **4b'** [(**L4**)$_2$Zn], whose identities were confirmed by their independent synthesis by addition of two equiv. of **L2H** or **L4H** to diethylzinc (Fig. S111, SI). The structure of the homoleptic complex **4b'** was further confirmed by X-Ray diffraction study and the ORTEP view is presented on Fig. 7. In order to examine the possibility that the homoleptic complexes could be involved in the above described polymerization reactions, they were tested as *rac*-lactide ROP catalysts. For comparative purposes, the homoleptic complex [(**L6**)$_2$Zn] (**6b'**) issued from the *N*-(*n*-propyl) FI ligand **L6H** was synthesized and tested in parallel (see Fig. S113 for ORTEP view of **6b'**, SI). The homoleptic complex **4b'**, when combined to isopropanol as co-initiator, afforded PLA with lower conversion than its heteroleptic counterpart (40% *vs* 80%; Table 4, entry 8 and Table 3, entry 4) and does not polymerize LA in the presence of lactic acid. Remarkably, the FI-Zn homoleptic complex **6b'** does not polymerize LA in the same conditions

Table 4. ROP of lactide mediated by FA-Zn complexes 2b, 2b', 4b and 4b'[a,b]

Entry	Init.	Co-init.	[*rac*-LA]:[Zn]$_0$:[co-init.]	Time	Conv (%)[c]	$M_{n,\,exp}$[d]	$M_{n,\,theo}$[e]	Đ[d]	P_r[f]
1	**2b**	^{i}PrOH+Lactic acid	100:1:1:1	40'	88	7 300	12 700	1.11	n.d.
2	**2b**	^{i}PrOH	100:1:1	40'	60	8 000	8 600	1.08	n.d.
3	**2b**	Lactic acid	100:1:1	40'	56	9 900	8 100	1.11	n.d.
4	**2b**	-	100:1	40'	10	n.d.	n.d.	n.d.	n.d.
5	**2b**	Lactic acid	100:1:1	2 h	96	13 300	13 800	1.22	0.63
6	**2b**	Glycolic acid	100:1:1	2 h	72	10 800	10 400	1.83	0.75
7	**2b**	Mandelic acid	100:1:1	2 h	92	15 500	13 300	1.29	0.63
8	**4b'**	^{i}PrOH	100:1:1	2 h	40	4 200	5 800	1.06	n.d.
9	**4b'**	Lactic acid	100:1:1	2 h	0	-	-	-	-
10	**6b'**	^{i}PrOH	100:1:1	2 h	0	-	-	-	-
11	**6b'**	Lactic acid	100:1:1	2 h	0	-	-	-	-
12	**2b'**	^{i}PrOH	100:1:1	2 h	97	9 900	14 000	1.11	0.55
13	**2b'**	Lactic acid	100:1:1	2 h	72	10 400	10 400	1.09	0.75
14	**2b**	^{i}PrOH	1000:1:10	2 h	63	9 500	9 100	1.11	n.d.
15	**2b'**	^{i}PrOH	1000:1:10	2 h	69	7 500	9 900	1.16	n.d.
16	**2b**	^{i}PrOH	1000:1:1	4 h	83	119 600	34 700	1.21	n.d
17	**2b'**	^{i}PrOH	1000:1:1	4 h	61	87 900	22 800	1,18	n.d.

[a] Polymerization conditions: [*rac*-LA]$_0$ = 1.5 M, CH_2Cl_2, 25°C. [b] Reactions performed with a batch of recrystallized and sublimed LA. [c] Monomer conversion. [d] Measured by GPC in THF (30°C) using PS standards and corrected by applying the appropriate correcting factor (0.58).[e] Calculated using $M_{n,theo}$ = [*rac*-LA]$_0$/[Zn]$_0$ × M_{LA} × conversion. [f] Determined from the methine region of the HD ^{1}H NMR spectrum. Note: the ratio [*rac*-LA]:[Zn]$_0$:[co-init.] is determined with respect to the number of equivalent per Zn center.

either in the presence of ^{i}PrOH or lactic acid. Species **2b'** achieved higher conversion than **2b** within 2 h, when using isopropanol as co-initiator (97% *vs* 93%; Table 4, entry 12 and Table 3). Conversely, in the presence of lactic acid, lactide ROP by **2b'** proceeded with lower conversion than with **2b**, but furnished PLA with higher heterotacticity (72% *vs* 96%, P_r = 0.75 *vs* 0.63, Table 4, entries 13 and 5). This trend was further confirmed by comparing the kinetics of the reaction within a shorter reaction time (20', Fig. 8). While **2b** showed a similar rate constant ($k_{app} \approx 0.03$ min^{-1}) with each co-initiator, **2b'** shows an approximately 4-fold higher rate constant with isopropanol than with lactic acid as co-initiators (k_{app} = 0.061 ± 0.006 vs 0.016 ± 0.004 min^{-1}), which makes it more active than **2b** in the first case and less in the second case. The evolution of the M_n and PDI values with conversion confirmed the well-controlled character of the polymerization with both complexes (Fig. 8). Noteworthy, the MALDI-ToF spectrum obtained from **2b'** and lactic acid as co-initiator differs from that of **2b** showing only one series with a peak spacing of 144 Da and peak mass with lactic acid end groups (Fig. 9). Finally, complexes **2b** and **2b'** were tested under immortal conditions in the presence of excess ^{i}PrOH and with a lower catalyst loading {[*rac*-LA]:[init]:[^{i}PrOH] = 1000:1:10}. Both catalysts **2b** and **2b'** gave PLA in 63 and 69% conversions (Table 4, entries 14 and 15), respectively, while maintaining good control over the molecular weight distributions. On the other hand, complexes **2b** and **2b'** yielded PLA with lower masses than expected using low catalyst and ^{i}PrOH loadings (Table 4, entries 16 and 17). Overall, the activities in solution displayed by **2b** and **2b'** are in the range of those of the most active FI complexes previously reported by Jones (k_{app} = 0.08 min^{-1}, [M]/[I] = 100/1, toluene, 80°C),[2h] Lin (k_{app} = 0.12 min^{-1}, [M]/[I] = 100/1, toluene, 25°C)[2c] and Darensbourg (k_{app} = 0.04 min^{-1}, [M]/[I] = 50/1, $CHCl_3$, 25°C)[15d], or to that of the robust bisguanidine Zn complex developed by Herres-Pawlis (k_{app} = 0.03 min^{-1}, [M]/[I] = 1000/1, toluene, 100°C).[10b]

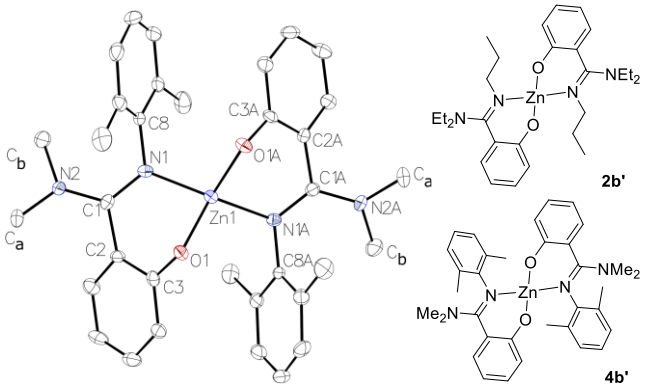

Figure 7. RHS: Representation of complexes **2b'** and **4b'**. LHS: ORTEP view of complex **4b'**. Hydrogen atoms are omitted for clarity. Selected distances (Å) and angles (°) of: C1–N1 1.321(4), C1–N2 1.350(4), Zn1-O1 1.934(2), Zn1-O1A 1.933(2), Zn1-N1 2.027(3), Zn1-N1A 2.022(3). Thermal ellipsoids are drawn at 50% probability level.

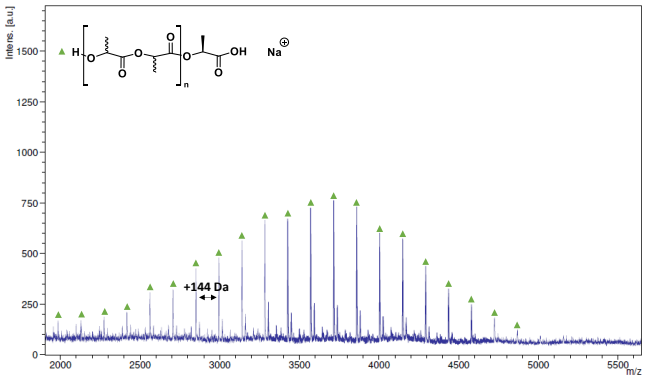

Figure 9. MALDI-TOF spectra of PLA produced using **2b'** with lactic acid as initiator (20°C, 20 min, 100:1:1)

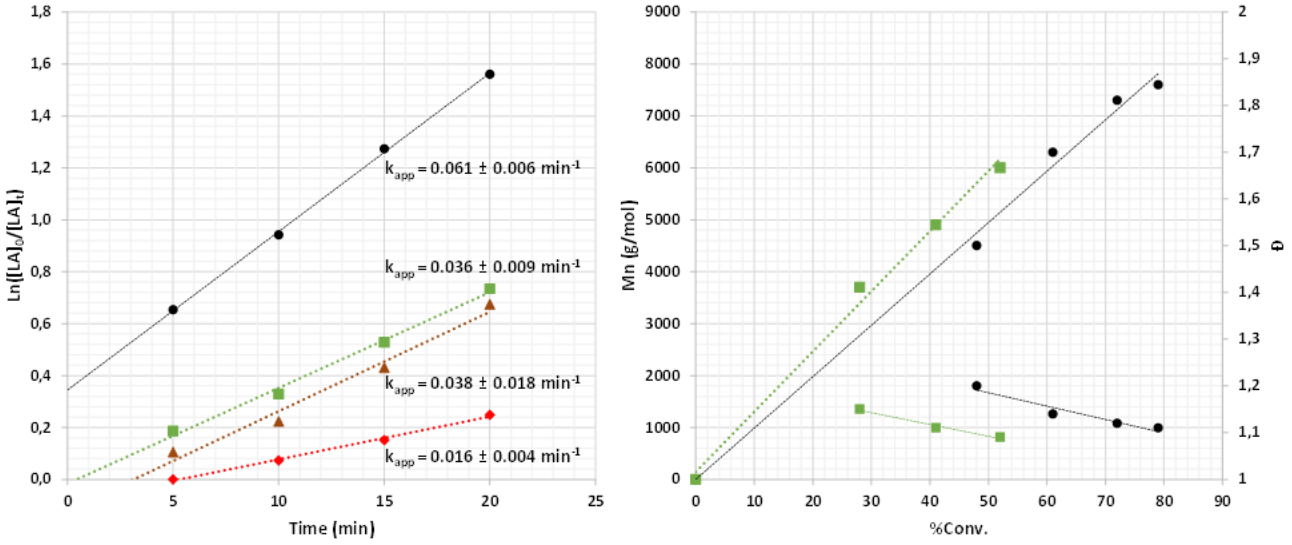

Figure 8. Left: First-order logarithmic plot for the polymerization of *rac*-LA at 20°C in DCM using **2b'** with ^{i}PrOH (●), lactic acid (◆) and **2b** with ^{i}PrOH (■), lactic acid (▲) as initiator (100:1:1). Right: M_n and PDI against conversion associated with the kinetic studies of **2b'** with ^{i}PrOH (●) and **2b** with ^{i}PrOH (■).

In conclusion, we have described a new generation of phenoxy-amidine ligand based on the FI scaffold, but for which the imine function has been replaced by a more robust and basic trisubstituted amidine. Five new phenoxy-amidine ligands have been synthesized *via* Vilsmeier-amidination reaction. In the solid state, the proligands feature an amidine moiety in *trans*-configuration and oriented orthogonally with respect to the aryloxy plane. Upon coordination, amidine has undergone isomerization from *trans* to *cis*-configuration, which enables the formation of chelate complexes of Al and Zn metal ions. These complexes have been trialed for the ROP of *rac*-lactide. Overall, Zn complexes surpass their Al counterparts, and complexes **2b**/**2b'**, featuring a trialkyl-substituted amidine, demonstrated the best performance. Remarkably, ROP catalytic activity is retained in a controlled manner even in the presence of lactic acid as a co-initiator allowing the production of well-defined PLA. In contrast, analogous FI or *N*-aryl FA Zn complexes showed no activity under similar conditions. This discrepancy might be explained by considering the highly basic character of the amidine function in **2b**/**2b'**, that may contribute to a better anchoring of the ligand and afford a more robust complex. Further studies to extend the scope of FA ligands and use them for the ROP of LA in industrially relevant conditions are currently underway.

EXPERIMENTAL SECTION

General consideration. All reactions, except when indicated, were carried out under an atmosphere of argon using conventional Schlenk techniques and Ar glovebox. DCM, diethyl ether, THF, toluene, and pentane were dried using a MBRAUN SPS 800. Analyses were performed at the "Plateforme d'Analyses Chimiques de Synthèse Moléculaire de l'Université de Bourgogne". Elemental analyses were performed by Mr Marcel Soustelle and Ms Tiffanie Régnier on CHNS ThermoFisher Scientific Flash EA 1112 analyzer. A satisfactory elemental analysis could not be obtained notably in case of complexes **2a**, **3a**, **1b** and **2b**, possibly due to partial hydrolysis of the compound outside the glovebox during the analysis process. Reagents were commercially available and used as received. High resolution mass spectra were recorded on a Thermo LTQ Orbitrap XL ESI-MS (ElectroSpray Ionization Mass Spectrometry). All X-Ray experimental procedure and crystal data are detailed in SI. NMR spectra (^{1}H, ^{13}C) were recorded on Bruker 300 Avance Neo, Bruker 400 Avance Neo, Bruker 500 Avance Neo, or Bruker 600 Avance HD spectrometers. All acquisitions were performed at 298 K. Chemical shifts are quoted in parts per million (δ) relative to TMS (for ^{1}H and ^{13}C). For ^{1}H and ^{13}C spectra, values were determined by using solvent residual signals (*e.g.* $CHCl_3$ in $CDCl_3$) as internal standards. The apparent multiplicity of the ^{1}H signals is reported. Assignment of ^{1}H and ^{13}C signals (when possible) was done through the use of 2D experiences (COSY, HSQC and HMBC). Nomenclature: the positions of carbon and hydrogen atoms in the aromatic rings of FA ligands were labelled according to Figure 10.

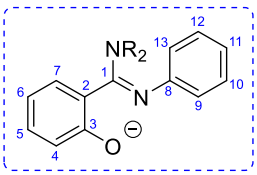

Figure 10. Numbering of C / H atoms in FA ligands.

Synthesis of 2-hydroxy-*N*,*N*-dimethyl-*N'*-(*n*-propyl)benzamidine (L1H). 896 mg (3.5 mmol, 1 eq.) of 2-(benzyloxy)-*N*,*N*-dimethylbenzamide were solubilized into 20 mL of dried toluene. The solution was cooled to 0°C and 0.3 mL (3.5 mmol, 1 eq.) of oxalyl chloride were added. The mixture was allowed to reach r.t. and heated at 60°C overnight. The volatiles were evaporated and the sticky residue was washed three times with 10 mL of diethyl ether before being taken back into 2 mL of dried CH_2Cl_2. 10 mL of dried diethyl ether were added to precipitate the residue, which was separated from the supernatant by cannula. The product was further washed with 10 mL of diethyl ether and then dried under vacuum before being taken back into 20 mL of dried CH_2Cl_2. The solution was cooled to 0°C and 1.4 mL (17.5 mmol, 5 eq.) of *n*-propylamine were added. The mixture was allowed to reach r.t. and stirred overnight. After hydrolysis with 20 mL of a 1M NaOH aqueous solution, the product was extracted three times with 25 mL of CH_2Cl_2, and the organic phases were combined, dried over $MgSO_4$ and evaporated under vacuum. The crude product was taken back into 10 mL of distilled water and a 1M HCl aqueous solution was added dropwise until pH=1. The aqueous phase was washed three times with 5 mL of diethyl ether and a 1M NaOH aqueous solution was added until pH=14. The amidine was then extracted three times with 40 mL of CH_2Cl_2. The organic phases were combined, dried over $MgSO_4$ and evaporated under vacuum. An hydrogenation overnight over 10 bar of H_2 on Pd/C 10% (15 w% of the crude amidine obtained) in 10 mL of ethanol followed by filtration and evaporation of the solvent afforded 300 mg of pure **L1H** (42% yield). **Elemental Analysis:** calcd. for $C_{12}H_{18}N_2O$: C, 69.87; H, 8.80; N, 13.58. Found: C, 69.84; H, 9.12; N, 12.87. **^{1}H NMR** (400.16 MHz, CD_2Cl_2, 298 K): δ (ppm) = 11.86 (s, 1H, O*H*), 7.14 (ddd, *J* = 8.7, 7.1, 1.9 Hz, 1H, H5), 6.83 (dd, *J* = 7.5, 1.9 Hz, 1H, H7), 6.78 (d, *J* = 11.7 Hz, 1H, H4), 6.52 (t, *J* =7.3 Hz, 1H, H6), 3.01 (overlapping signals, 8H, N*Me*$_2$ + NC*H*$_2$CH$_2$CH$_3$), 1.47 (hex, *J* = 6.9 Hz, 2H, NCH$_2$C*H*$_2$CH$_3$), 0.77 (t, *J* = 7.4 Hz, 3H, NCH$_2$CH$_2$C*H*$_3$). **{^{1}H}^{13}C NMR** (100.63 MHz, CD_2Cl_2, 298 K): δ(ppm) = 165.64 (C1), 163.12 (C3), 131.81 (C5), 128.74 (C7), 119.88 (C4), 118.43 (C2), 113.85 (C6), 49.76 (N*C*H$_2$CH$_2$CH$_3$), 39.99 (N*Me*$_2$), 24.77 (NCH$_2$*C*H$_2$CH$_3$), 11.40 (NCH$_2$CH$_2$*C*H$_3$).

Synthesis of *N*,*N*-diethyl-2-hydroxy-*N'*-(*n*-propyl)benzamidine (L2H). This compound was prepared similarly to **L1H**, starting with 2-(benzyloxy)-*N*,*N*-diethylbenzamide (1 g, 3.53 mmol). **L2H** was isolated as a white solid (273 mg, 33% yield). **Elemental Analysis:** calcd for $C_{14}H_{22}N_2O$: C, 71.76; H, 9.46; N, 11.95. Found: C, 71.58; H, 9.07; N, 11.72. **^{1}H NMR** (499.87 MHz, $CDCl_3$)**:** δ (ppm) = 7.16 (t, *J* = 7.2 Hz, 1H, H5), 6.79 (d, *J* = 7.9 Hz, 2H, H7 + H4), 6.46 (t, *J* = 7.2 Hz, 1H, H6), 3.46 (br, 4H, NC*H*$_2$CH$_3$), 3.05 (t, *J* = 7.4 Hz, 2H, NC*H*$_2$CH$_2$CH$_3$), 1.49 (m, 2H, NCH$_2$C*H*$_2$CH$_3$), 1.19 (t, *J* = 6.9 Hz, 6H, NCH$_2$C*H*$_3$), 0.73 (t, *J* = 7.4 Hz, 3H, NCH$_2$CH$_2$C*H*$_3$). **{^{1}H}^{13}C NMR** (125.70 MHz, $CDCl_3$): δ (ppm) = 164.52 (C1), 163.68 (C3), 131.62 (C5), 127.84 (C4), 120.32 (C7), 117.49 (C2), 112.46 (C6), 48.49 (N*C*H$_2$CH$_2$CH$_3$), 44.19 (N*C*H$_2$CH$_3$), 24.12 (NCH$_2$*C*H$_2$CH$_3$), 13.16 (NCH$_2$*C*H$_3$), 11.46 (NCH$_2$CH$_2$*C*H$_3$).

Synthesis of *N*,*N*-diethyl-2-hydroxy-*N'*-(*n*-propyl)benzamidinium bromide [L2H$_2$][Br]. To a solution of **L2H** (25 mg, 0.1 mmol) in dichloromethane (2 mL), aqueous HBr was added (1 mL, 0.1M) at 0°C. After stirring 30 min at r.t., $MgSO_4$ was added. Further filtration and drying under vacuum gave **[L2H$_2$][Br]** in quantitative yield. **Elemental Analysis:** calcd for $C_{14}H_{23}BrN_2O$: C, 53.34; H, 7.35; N, 8.89. Found: C, 53.14; H, 7.56; N, 8.73. **HR-MS (ESI-pos):** calcd for $[C_{14}H_{23}N_2O]^+$ [M - Br]$^+$: 235.18049. Found: 235.17943 (-4.5 ppm). **^{1}H NMR** (300.13 MHz, $CDCl_3$): δ (ppm) = 9.69 (s, 1H, OH), 9.23 (t, *J* = 6.2 Hz, 1H, NH), 7.69 (d, *J* = 8.2 Hz, 1H, H4), 7.40 (ddd, *J* = 8.4, 6.2, 2.9 Hz, 1H, H5), 7.02-6.91 (overlapping signals, 2H, H7 + H6), 3.91 (m, 2H, NC*H*$_2$CH$_3$), 3.30-3.14 (overlapping signals, 3H, NC*H*$_2$CH$_3$ + NC*H*$_2$CH$_2$CH$_3$), 2.98-2.84 (m, 1H, NC*H*$_2$CH$_2$CH$_3$), 1.80-1.48 (m, 2H, NCH$_2$C*H*$_2$CH$_3$), 1.38 (t, *J* = 7.1 Hz, 3H, NCH$_2$C*H*$_3$), 1.08 (t, *J* = 7.1 Hz, 3H, NCH$_2$C*H*$_3$), 0.71 (t, *J* = 7.4 Hz, 3H, NCH$_2$CH$_2$C*H*$_3$). **{^{1}H}^{13}C NMR** (75.47 MHz, $CDCl_3$): δ (ppm) = 162.30 (C1), 154.39 (C3), 133.36 (C5), 127.09 (C7), 119.96 (C6), 118.12 (C4), 114.34 (C2), 47.51 (NCH$_2$CH$_2$CH$_3$), 47.42 (N*C*H$_2$CH$_3$), 44.00 (N*C*H$_2$CH$_3$), 23.37 (NCH$_2$*C*H$_2$CH$_3$), 13.77 (NCH$_2$*C*H$_3$), 12.05 (NCH$_2$*C*H$_3$), 11.24 (NCH$_2$CH$_2$*C*H$_3$).

2-hydroxy-*N*,*N*-dimethyl-*N'*-phenylbenzamidine (L3H). Under argon, 1.0 g (5.58 mmol) of 2-methoxy-*N*,*N*-dimethylbenzamide was solubilized in 30 mL of dried toluene. The solution was cooled to 0°C and 0.73 mL (8.37 mmol, 1.5 eq.) of oxalyl chloride were added. The mixture was allowed to reach r.t. and then heated at 60°C for two days. After cooling the solution to r.t., the volatiles were evaporated under

vacuum. The residue was taken back into 20 mL of dried toluene affording a sticky residue. The supernatant was cannulated, and 20 mL of dried toluene and 20 mL of dried diethyl ether were added. The suspension was stirred for 2 h and then concentrated by evaporation. The supernatant was cannulated and the whitish solid was then washed successively with 20 mL of toluene and 20 mL of diethyl ether. The white powder was then dried under vacuum before being solubilized into 40 mL of dried dichloromethane. The solution was cooled to 0°C and then 3.9 mL (27.90 mmol, 5 eq.) of triethylamine and 0.6 mL (6.70 mmol, 1.2 eq.) of aniline were successively slowly added. The solution was allowed to reach r.t. and then stirred for 3 h. After hydrolysis with 40 mL of a 1M aqueous solution of NaOH, the product was extracted three times with 40 mL of dichloromethane. The organic phases were combined, dried over $MgSO_4$ and evaporated under vacuum, affording a brown oil. The residue was solubilized into 35 mL of dichloromethane and 22.3 mL of a 1M solution of BBr_3 in dichloromethane were slowly added at 0°C. The mixture was allowed to reach r.t. and stirred overnight. Volatiles were evaporated under vacuum, and the obtained residue was taken back into 30 mL of dichloromethane. A 1M aqueous solution of NaOH was slowly added until pH=8. Dichloromethane was evaporated, and the aqueous suspension was filtrated. The whitish powder was dried under vacuum, affording 790 mg of **L3H** (59 % yield). **Elemental Analysis:** calcd. for $C_{15}H_{16}N_2O$: C, 74.97; H, 6.71; N, 11.66. Found: C, 74.53; H, 6.85; N, 11.27. **^{1}H NMR** (400.16 MHz, MeOD, 298 K): δ (ppm) = 7.03 (ddd, *J* =8.7, 7.3, 1.8 Hz, 1H, H5), 7.01-6.94 (m, 2H, H10), 6.82-6.72 (m, 4H, H7 + 2H9 + H11), 6.69 (dd, *J* = 8.3, 1.0 Hz, 1H, H4), 6.56 (td, *J* = 7.4, 1.0 Hz, 1H, H6), 3.03 (s, 6H, NMe_2). **{^{1}H}^{13}C NMR** (150.94 MHz, MeOD, 298 K): δ (ppm) = 163.16 (C1), 157.64 (C3), 150.31 (C8), 131.55 (C5), 130.42 (C7), 129.05 (C10), 124.63 (C9), 123.48 (C11), 122.06 (C2), 119.28 (C6), 117.08 (C4), 38.65 (NMe_2).

2-hydroxy-*N*,*N*-dimethyl-*N*'-(2,6-dimethylphenyl)benzamidine (L4H) This compound was prepared similarly to **L3H**, starting with 2-methoxy-*N*,*N*-dimethylbenzamide (0.95 g, 5.3 mmol) and using 0.79 mL (6.4 mmol, 1.2 eq.) of 2,6-dimethylaniline. **L4H** was isolated as a white solid (585 mg, 41 % yield). **Elemental Analysis:** calcd. for $C_{17}H_{20}N_2O$: C, 76.09; H, 7.51; N, 10.44. Found: C, 76.35; H, 7.98; N, 10.23. **^{1}H NMR** (400.16 MHz, MeOD, 298 K): δ (ppm) = 7.04 (td, *J* = 7.8, 1.6 Hz, 1H, H5), 6.83-6.66 (overlapping signals, 5H, H4 + H7 + H10/12 + H11), 6.50 (t, *J* = 7.5 Hz, 1H, H6), 3.11 (s, 6H, NMe_2), 2.18 (s, 6H, C9/13-CH_3). **{^{1}H}^{13}C NMR** (100.63 MHz, MeOD, 298 K): δ (ppm) = 162.01 (C1), 156.92 (C3), 145.94 (C8), 132.87 (C9), 131.96 (C5), 129.52 (C7), 128.56 (C10), 124.41 (C11), 120.59 (C2), 118.97 (C6), 117.44 (C4), 39.99 (NMe_2), 18.92 (C9-CH_3).

Synthesis of *N*,*N*-diethyl-2-hydroxy-*N*'-phenylbenzamidine (L5H) This compound was prepared similarly to **L3H**, starting with *N*,*N*-diethyl-2-methoxybenzamide (2.0 g, 9.66 mmol) and using 1.06 mL (11.6 mmol, 1.2 eq.) of aniline. **L5H** was isolated as whitish powder (1.61 g, 62% yield). **Elemental Analysis:** calcd. for $C_{17}H_{20}N_2O$: C, 76.09; H, 7.51; N, 10.44. Found: C, 75.82; H, 7.90; N, 10.06. **^{1}H NMR** (400.16 MHz, CD_2Cl_2, 298 K): δ (ppm) = 7.14 (td, *J* = 7.8, 1.5 Hz, 1H, H4), 7.05-6.99 (m, 2H, H9/H10), 6.99-6.93 (m, 1H, H11), 6.81-6.72 (m, 3H, H5 + H6 + H7), 6.61 (d, *J* = 7.6 Hz, 2H, H10/H9), 3.37 (br, 4H, CH_2CH$_3$), 1.16 (t, *J* = 7.1 Hz, 6H, CH$_2$CH_3). **{^{1}H}^{13}C NMR** (100.63 MHz, CD_2Cl_2, 298 K): δ(ppm) = 157.50 (C1), 153.95 (C3), 151.39 (C8), 131.2 (C4), 130.59 (C11), 128.98 (C9/C10), 122.93 (C10/C9), 122.19 (C5/C6/C7), 121.41 (C2), 120.57 (C5/C6/C7), 113.56 (C5/C6/C7), 43.12 (*C*H$_2$CH$_3$), 13.84 (CH$_2$*C*H$_3$).

Synthesis of 1a: In a glovebox, 61.9 mg (0.3 mmol) of **L1H** were suspended into 3 mL of THF. Then 0.15 mL (0.3 mmol, 1 eq.) of a 2M solution of $AlMe_3$ in hexane were added and the solution was stirred at r.t. for 2 h. Volatiles were evaporated under vacuum, and the sticky oil obtained was taken back in 4 mL of pentane. The solvent was then evaporated and 3 mL of pentane were added and further evaporated. 3 mL of pentane were used to suspend the white solid obtained. After decantation, the supernatant was eliminated and the white powder dried under vacuum, affording 29 mg (37% yield) of complex **1a** containing about 9% of $AlMe_3$. **Elemental Analysis:** calcd. for $(C_{14}H_{23}AlN_2O)_{91}(Al(CH_3)_3)_9$: C, 63.73; H, 8.94; N, 10.40. Found: C, 63.28; H, 8.69; N, 10.28. **^{1}H NMR** (400.16 MHz, THF-D_8, 298 K): δ (ppm) = 7.40-7.16 (overlapping signals, 2H, H5+H7), 6.78 (d, *J* = 8.3 Hz, 1H, H4), 6.66 (t, *J* = 7.6 Hz, 1H), 3.50 (br, 2H, NCH_2CH$_2$CH$_3$), 3.01 (s, 6H, NMe_2), 1.67 (m, 2H, NCH$_2$CH_2CH$_3$), 0.99 (t, 3H, NCH$_2$CH$_2$CH_3), -0.98 (6H, s, AlMe_2). **{^{1}H}^{13}C NMR** (100.63 MHz, THF-D_8, 298 K): δ (ppm) = 170.08 (C1), 166.59 (C3), 134.55 (C5), 132.48 (C7), 123.28 (C4), 119.19 (C2), 116.79 (C6), 50.85 (NCH_2CH$_2$CH$_3$), 43.10 (NMe_2), 24.45 (NCH$_2$CH_2CH$_3$), 11.96 (NCH$_2$CH$_2$CH_3), -0.98 (AlMe_2).

Synthesis of 2a: This compound was prepared similarly to **1a**, using **L2H** (187 mg, 0.8 mmol) and $AlMe_3$ 2M/hexanes (1 eq., 0.8 mmol, 0.4 mL). **2a** was obtained as a white solid (167 mg, 72% yield). **Elemental Analysis:** calcd. for $C_{16}H_{27}AlN_2O$: C, 66.18; H, 9.37; N, 9.65. Found: C, 63.88; H, 9.49; N, 9.38. **^{1}H NMR** (499.87 MHz, CD_2Cl_2, 298 K): 7.32 (overlapping signals, 2H, H5 + H4), 6.86 (d, *J* = 8.5 Hz, 1H, H7), 6.75 (t, *J* = 8.0 Hz, 1H, H6), 3.49-3.45 (m, 2H, NCH_2CH$_2$CH$_3$), 3.33 (q, *J* = 7.0 Hz, 4H, NCH_2CH$_3$), 1.81-1.71 (m, 2H, NCH$_2$CH_2CH$_3$), 1.18 (t, *J* = 7.0 Hz, 6H, NCH$_2$CH_3), 1.02 (t, *J* = 7.5 Hz, 3H, NCH$_2$CH$_2$CH_3), -0.93 (s, 6H, $AlMe_2$). **{^{1}H}^{13}C NMR** (125.70 MHz, CD_2Cl_2, 298 K): 170.19 (C1), 166.13 (C3), 134.99 (C5), 132.99 (C4), 123.35 (C7), 119.58 (C2), 117.62 (C6), 52.17 (NCH_2CH$_2$CH$_3$), 46.56 (NCH_2CH$_3$), 24.06 (NCH$_2$CH_2CH$_3$), 14.01 (NCH$_2$CH_3), 12.8 (NCH$_2$CH$_2$CH_3), -10.85 ($AlMe_2$).

Synthesis of 3a: This compound was prepared similarly to **1a**, using **L3H** (144.2 mg, 0.6 mmol) and $AlMe_3$ 2M/hexanes (1 eq., 0.3 mL, 0.6 mmol). **3a** was obtained as a white solid (113 mg, 63% yield). **Elemental Analysis:** calcd. for $C_{17}H_{21}AlN_2O$: C, 68.90; H, 7.14; N, 9.45. Found: C, 67.20; H, 6.86; N, 9.15. **^{1}H NMR** (400.16 MHz, CD_2Cl_2, 298 K): δ (ppm) = 7.45-7.37 (overlapping signals, 4H, H5 + H7 + H10/12), 7.25 (tt, *J* = 7.5, 1.1 Hz, 1H, H11), 7.06-7.00 (m, 2H, H9/13), 6.93 (d, *J* = 8.1 Hz, 1H, H4), 6.80 (td, *J* = 7.6, 1.1 Hz, 1H, H6), 2.70 (s, 6H, NMe_2), -1.17 (s, 6H, $AlMe_2$). **{^{1}H}^{13}C NMR** (100.63 MHz, CD_2Cl_2, 298 K): δ(ppm) = 167.70 (C1), 166.13 (C3), 145.53 (C8), 135.31 (C5/C7), 132.52 (C5/C7), 129.84 (C10), 126.06 (C11), 125.01(C9), 123.38 (C4), 118.12 (C2), 117.25 (C6), 44.10 (NMe_2), -11.18 ($AlMe_2$).

Synthesis of 4a: This compound was prepared similarly to **1a**, using **L4H** (161.0 mg, 0.6 mmol) and $AlMe_3$ 2M/hexanes (1 eq., 0.3 mL, 0.6 mmol). **3a** was obtained as a whitish powder (128 mg, 66% yield). **Elemental Analysis:** calcd. for $C_{19}H_{25}AlN_2O$: C, 70.35; H, 7.77; N, 8.32. Found: C, 69.95; H, 8.09; N, 8.71. **^{1}H NMR** (400.16 MHz, CD_2Cl_2, 298 K): δ (ppm) = 7.44-7.36 (m, 2H, H5 + H7), 7.14-7.03 (m, 3H, 2H10 + H11), 6.96 (dd, *J* = 8.3, 1.3 Hz, 1H, H4), 6.82 (ddd, *J* = 8.2, 7.1, 1.3 Hz, 1H, H6), 2.66 (s, 6H, NMe_2), 2.19 (s, 6H, C9-CH_3), -1.24 (s, 6H, $AlMe_2$). **{^{1}H}^{13}C NMR** (100.63 MHz, CD_2Cl_2, 298 K): δ(ppm) = 167.41 (C1), 166.21 (C3), 144.21 (C8), 135.00 (C5), 132.98 (C9), 132.34 (C7), 128.85 (C10), 126.07 (C11), 123.47 (C4), 118.16 (C2), 117.24 (C6), 42.93 (NMe_2), 19.16 (C9-CH_3), -11.55 ($AlMe_2$).

Synthesis of 5a: In a glovebox, **L5H** (268 mg, 1 mmol) was suspended in DCM (10 mL) and $AlMe_3$ 2M/hexanes (1 eq., 1 mmol, 0.5 mL) were added slowly. The mixture was stirred 2 h and then solvent was removed under vacuum. 10 mL of pentane were added and further removed to give 206 mg of **5a** as a white solid (64% yield). **Elemental Analysis:** calcd. for $C_{19}H_{25}AlN_2O$: C, 70.35; H, 7.77; N, 8.64. Found: C, 69.72; H, 8.02; N, 8.42. **^{1}H NMR** (400.16 MHz, CD_2Cl_2, 298 K): δ(ppm) = 7.44-7.34 (overlapping signals, 4H, H10/12 + H7 + H6), 7.25 (t, *J* = 7.5 Hz, 1H, H11), 7.10 (d, *J* = 8.5 Hz, 2H, H9), 6.93 (d, *J* = 8.0 Hz, 1H, H4), 6.79 (td, *J* = 7.6, 1.1 Hz, 1H, H5), 3.05 (q, *J* = 7.1 Hz, 4H, NCH_2CH$_3$), 1.05 (t, *J* = 7.1 Hz, 6H, NCH$_2$CH_3), -1.18 (s, 6H, $AlMe_2$). **{^{1}H}^{13}C NMR** (100.63 MHz, CD_2Cl_2, 298 K): δ (ppm) = 168.34 (C1), 166.58 (C3), 145.86 (C8), 135.58 (C6/C7), 133.05 (C7/C6), 130.28 (C10), 126.61 (C11), 125.15 (C9), 123.78 (C4), 119.29 (C2), 117.71 (C5), 46.82 (NCH_2CH$_3$), 13.15 (NCH$_2$CH_3), -10.90 ($AlMe_2$).

Synthesis of 1b: In the glovebox, 114.5 mg (0.56 mmol) of **L1H** was solubilized in THF (8 mL) and $ZnEt_2$ 1M/hexanes (1 eq., 0.56 mmol, 0.56 mL) was added slowly. The mixture was stirred 2 h and then solvent was removed under vacuum. 4 mL of pentane were added and after a few minutes of stirring, the suspension was let to settle and the supernatant was eliminated. The whitish solid was finally dried under vacuum, affording 91 mg of **1b** as a white solid (54% yield). **Elemental Analysis:** calcd. for $C_{14}H_{22}N_2OZn$: C, 56.10; H, 7.40; N, 9.35. Found: C, 53.45; H, 6.69; N, 8.96. **^{1}H NMR** (400.16 MHz, pyridine-D_5, 298 K): δ(ppm) = 7.35 (t, *J* = 7.3 Hz, 1H, H5), 7.19 (d *J* = 6.2 Hz, 1H, H7),

7.11 (d, *J* = 8.1 Hz, 1H, H4), 6.77 (t, *J* = 7.2 Hz, 1H, H6), 3.46 (br, 2H, NC*H*$_2$CH$_2$CH$_3$), 3.06 (6H, s, NMe$_2$), 1.76 (m, 2H, NCH$_2$C*H*$_2$CH$_3$), 1.67 (t, *J* = 8.1 Hz, 3H, ZnCH$_2$C*H*$_3$), 0.94 (t, *J* = 7.3 Hz, 3H, NCH$_2$CH$_2$C*H*$_3$), 0.83 (q, *J* = 8.1 Hz, 2H, ZnC*H*$_2$CH$_3$). **{^{1}H}^{13}C NMR** (100.63 MHz, pyridine-D$_5$, 298K): δ(ppm) = 166.28 (C3), 163.81 (C1), 130.32 (C5), 129.21 (C7), 126.42 (C2), 120.72 (C4), 113.92 (C6), 54.04 (NCH$_2$CH$_2$CH$_3$), 38.41 (NMe), 26.97 (NCH$_2$*C*H$_2$CH$_3$), 14.69 (ZnCH$_2$*C*H$_3$), 13.04 (NCH$_2$CH$_2$*C*H$_3$), -2.37 (Zn*C*H$_2$CH$_3$).

Synthesis of 2b: This compound was prepared similarly to **1b**, using **L2H** (187 mg, 0.8mmol) and ZnEt$_2$ 1M/hexanes (1 eq., 0.8 mmol, 0.8 mL). **2b** was obtained as a white solid (235 mg, 90% yield). **Elemental Analysis:** calcd. for C$_{16}$H$_{26}$N$_2$OZn: C, 58.63; H, 8.00; N, 8.55. Found: C, 57.64; H, 8.54; N, 8.18. **^{1}H NMR** (400.16 MHz, pyridine-D$_5$, 298 K): δ(ppm) = 7.31 (t, *J* = 7.4 Hz, 1H, H5), 7.21-7.18 (m, 1H, H7), 7.11 (d, *J* = 8.0 Hz, 1H, H4), 6.76 (dd, *J* = 7.3, 1.0 Hz, 1H, H6), 3.65 (br, 2H, NC*H*$_2$CH$_3$), 3.56-3.31 (overlapping signals, 4H, NC*H*$_2$CH$_3$ + NC*H*$_2$CH$_2$CH$_3$), 1.78-1.68 (m, 2H, NCH$_2$C*H*$_2$CH$_3$), 1.67 (q, *J* = 8.1 Hz, 3H, ZnCH$_2$C*H*$_3$), 1.19 (br, 6H, NCH$_2$C*H*$_3$), 0.94 (t, *J* = 7.3 Hz, 3H, NCH$_2$CH$_2$C*H*$_3$), 0.84 (q, *J* = 8.1 Hz, 2H, ZnC*H*$_2$CH$_3$). **{^{1}H}^{13}C NMR** (100.63 MHz, pyridine-D$_5$, 298 K): δ(ppm) =166.17 (C3), 162.16 (C1), 130.13 (C5), 129.37 (C7), 126.58 (C2), 120.06 (C4), 113.73 (C6), 53.72 (N*C*H$_2$CH$_2$CH$_3$), 42.16 (br, N*C*H$_2$CH$_3$), 26.98 (NCH$_2$*C*H$_2$CH$_3$), 14.79 (br, NCH$_2$*C*H$_3$), 14.67 (ZnCH$_2$*C*H$_3$), 13.11 (NCH$_2$CH$_2$*C*H$_3$), -2.31 (Zn*C*H$_2$CH$_3$).

Synthesis of 3b: This compound was prepared similarly to **1b**, using **L3H** (144 mg, 0.6 mmol) and ZnEt$_2$ 1M/hexanes (1 eq., 0.6 mmol, 0.6 mL). **3b** was obtained as a whitish solid (130 mg, 65% yield). **Elemental Analysis:** calcd. for C$_{17}$H$_{20}$N$_2$OZn: C, 61.18; H, 6.04; N, 8.39. Found: C, 59.57; H, 6.12; N, 8.09. **^{1}H NMR** (400.16 MHz, CD$_2$Cl$_2$, 298 K): δ(ppm) = 7.42 (t, *J* = 7.8 Hz, 2H, H10), 7.25-7.14 (m, 2H, H7 + H11), 7.06 (d, *J* = 7.8 Hz, 2H, H9), 6.97 (ddd, *J* = 8.6, 7.0 Hz, 1.9 Hz, 1H, H5), 6.57 (td, *J* = 7.5, 1.0 Hz, 1H, H6), 5.45 (d, *J* = 8.3 Hz, 1H, H4), 2.61 (s, 6H, NMe$_2$), 0.94 (t, *J* = 8.1 Hz, 3H, ZnCH$_2$C*H*$_3$), -0.06 (q, *J* = 8.1 Hz, 2H, ZnC*H*$_2$CH$_3$). **{^{1}H}^{13}C NMR** (100.63 MHz, CD$_2$Cl$_2$, 298 K): δ(ppm) = 167.51 (C3), 165.11 (C1), 148.83 (C8), 133.04 (C5), 132.21 (C7), 129.37 (C10), 124.37 (C9), 124.07 (C11), 123.29 (C4), 120.91 (C2), 116.40 (C6), 43.21 (NMe$_2$), 13.31 (ZnCH$_2$*C*H$_3$), -2.87 (Zn*C*H$_2$CH$_3$).

Synthesis of 4b. This compound was prepared similarly to **1b**, using **L4H** (161.0 mg, 0.6 mmol) and ZnEt$_2$ 1M/hexanes (1 eq., 0.6 mmol, 0.6 mL). **4b** was obtained as a white solid (183 mg, 85% yield). **Elemental Analysis:** calcd. for C$_{19}$H$_{24}$N$_2$OZn: C, 63.08; H, 6.69; N, 7.74. Found: C, 62.47; H, 6.63; N, 7.47. **^{1}H NMR** (400.16 MHz, pyridine-D$_5$, 298 K): δ(ppm) = 7.17-7.00 (overlapping signals, 3H, H5 + H7 + H10/H12), 6.94-6.81 (overlapping signals, 2H, H4 + H10/H12), 6.74 (t, *J* = 7.5 Hz, 1H, H11), 6.43 (t, *J* = 7.3 Hz, 1H, H6), 3.21 (s, 6H, NMe$_2$), 2.56 (s, 3H, C9-C*H*$_3$ or C13-C*H*$_3$), 2.36 (s, 3H, C9-C*H*$_3$ or C13-C*H*$_3$), 1.62 (t, *J* = 8.0 Hz, 3H, ZnCH$_2$C*H*$_3$), 0.79 (q, *J* = 7.7 Hz, 2H, ZnC*H*$_2$CH$_3$). **{^{1}H}^{13}C NMR** (100.63 MHz, pyridine-D$_5$, 298 K): δ(ppm) = 165.93 (C3), 160.65 (C1), 151.58 (C8), 130.68 (C5), 129.89 (C9 + C13), 129.44 (C7), 128.31 (C10/C12), 127.74 (C10/C12), 124.99, (C2), 120.59 (C11), 120.32 (C4), 113.47 (C6), 38.45 (NMe$_2$), 19.93 (C9-*C*H$_3$ + C13-*C*H$_3$), 14.53 (ZnCH$_2$*C*H$_3$), -2.67 (Zn*C*H$_2$CH$_3$)

Synthesis of 5b: In the glovebox, **L5H** (1 eq., 0.5mmol, 135 mg) was suspended in CH$_2$Cl$_2$ (10 mL) and ZnEt$_2$ 1M/hexanes (1 eq., 0.5 mmol, 0.5 mL) were added slowly. The mixture was stirred 1 h and then solvent was removed under vacuum to give 140 mg of **5b** as a white solid (78% yield). **Elemental Analysis:** calcd. for C$_{19}$H$_{24}$N$_2$OZn: C, 63.08; H, 6.69; N, 7.74. Found: C, 62.26; H, 6.99; N, 7.55. **^{1}H NMR** (499.87 MHz, CD$_2$Cl$_2$, 298 K): δ(ppm) = 7.43 (t, *J* = 8.1 Hz, 2H, H10), 7.21 (t, *J* = 7.4 Hz, 1H, H11), 7.15 (d, *J* = 8.1 Hz, 3H, 2H9 + H7), 6.96 (ddd, *J* = 8.3, 7.1, 1.7 Hz, 1H, H5), 6.57 (td, *J* = 8.0, 1.7 Hz, 1H, H6), 5.47 (d, *J* = 8.3 Hz, 1H, H4), 2.96 (br, 4H, NC*H*$_2$CH$_3$), 1.03 (t, *J* = 7.1 Hz, 6H, NCH$_2$C*H*$_3$), 0.94 (t, *J* = 8.1 Hz, 3H, ZnCH$_2$C*H*$_3$), -0.04 (q, *J* = 8.1 Hz, 2H, ZnC*H*$_2$CH$_3$). **{^{1}H}^{13}C NMR** (125.70 MHz, CD$_2$Cl$_2$, 298 K): δ(ppm) = 167.89 (C1), 165.20 (C3), 149.15 (C8), 133.19 (C5), 132.69 (C9/C13), 129.77 (C10/C12), 124.55 (C11), 124.46 (C7), 123.59 (C4), 121.91 (C2), 116.80 (C6), 45.65 (N*C*H$_2$CH$_3$), 13.60 (ZnCH$_2$*C*H$_3$), 12.98 (NCH$_2$*C*H$_3$), -2.42 (Zn*C*H$_2$CH$_3$).

Synthesis of 2b': In the glovebox, 234 mg (1 mmol) of **L2H** was solubilized in THF (8 mL) and ZnEt$_2$ 1M/hexanes (0.5 eq., 0.5 mmol, 0.5 mL) was added slowly. The mixture was stirred 2 h and then solvent was removed under vacuum affording 250 mg of **2b'** as a white solid (94% yield). **Elemental Analysis:** calcd. for C$_{28}$H$_{42}$N$_4$O$_2$Zn: C, 63.21; H, 7.96; N, 10.53. Found: C, 61.31; H, 7.64; N, 10.11. **^{1}H NMR** (400.16 MHz, pyridine-D$_5$, 298 K): δ(ppm) = 7.07-7.01 (m, 3H, H$_{Ar}$), 6.61 (s, 1H, H$_{Ar}$), 3.47-3.21 (overlapping signals, 6H, NC*H*$_2$), 1.59-1.57 (br, 2H, NCH$_2$C*H*$_2$CH$_3$), 1.06 (br, 6H, NCH$_2$C*H*$_3$), 0.78 (br, 3H, NCH$_2$CH$_2$C*H*$_3$). **{^{1}H}^{13}C NMR** (100.6 MHz, 298K, Pyridine-D5): 164.53(Cq), 161.68 (Cq), 130.27 (CH$_{Ar}$), 129.21 (CH$_{Ar}$), 126.2 (Cq), 120.18 (CH$_{Ar}$), 114.79 (CH$_{Ar}$), 53.38 (N*C*H$_2$CH$_2$CH$_3$), 42.22 (N*C*H$_2$CH$_3$), 34.52 (NCH$_2$*C*H$_2$CH$_3$), 14.50 (NCH$_2$*C*H$_3$), 12.88 (NCH$_2$CH$_2$*C*H$_3$).

Synthesis of 4b': In the glovebox, 161 mg (0.6 mmol) of **L4H** was solubilized in THF (8 mL) and ZnEt$_2$ 1M/hexanes (0.5 eq., 0.3 mmol, 0.3 mL) was added slowly. The mixture was stirred 2 h and then solvent was removed under vacuum. The white solid was washed with pentane and dried affording 137 mg of **4b'** (76% yield). **Elemental Analysis:** calcd. for C$_{34}$H$_{38}$N$_4$O$_2$Zn: C, 68.05; H, 6.38; N, 9.34. Found: C, 68.28; H, 5.97; N, 9.21. **^{1}H NMR** (400.16 MHz, CD$_2$Cl$_2$, 298 K): δ(ppm) = 7.04 (bs, 1H, H10 or H12), 7.00 (dd, J = 7.90, 1.80 Hz, 1H, H7), 6.83-6.79 (overlapping signals, 2H, H5 + H11), 6.58 (bs, 1H, H12 or H10), 6.41 (t, *J* = 7.36 Hz, 1H, H6), 6.00 (d, *J* = 8.35 Hz, 1H, H4), 2.50 (bs, 6H, NMe$_2$), 2.19 (bs, 3H, C-C*H*$_3$), 1.78 (bs, 3H, C-C*H*$_3$). **{^{1}H}^{13}C NMR** (100.6 MHz, 298 K, CD$_2$Cl$_2$): 171.70 (C3), 167.55 (C1), 146.25 (C9), 133.43 (C5), 132.20 (C7), 131.89 (C9 or C13), 131.52 (C13 or C9), 128.26 (C10 or C12), 128.47 (C12 or C10), 124.84 (C11), 123.99 (C4), 118.93 (C2), 113.92 (C6), 42.51 (NMe$_2$), 12.09 (C-*C*H$_3$).

Polymer synthesis procedure: Under argon, 288.03 mg (2.00 mmol) of *rac*-Lactide and 0.01 eq. of catalyst are weighed in a vial then mixed in the chosen solvent. Afterwards, 0.01 eq. of co-initiator is added with a 5µL Hamilton then the vial is crimped and let stirred at the desired temperature.

Gel Permeation analysis: The number-average, weight-average masses (M_n and M_w respectively) and molar distribution (M_w/M_n) of the polyester samples were determined by size exclusion chromatography at 30°C with the Agilent 1260 Infinity system equipped with Varian 390-LC refractometer detector. Tetrahydrofuran (THF) was used as the eluent and the flow rate was set up at 1.0 mL/min. A 5 µm pre-column and two aligned Polypore 5 µm (7.5 × 300 mm) were used. Calibration were performed using polystyrene standards (900-1 000 000 g/mol) and raw values of M_n were thus obtained.

MALDI-ToF analysis: Mass spectra were acquired on a time-of-flight mass spectrometer (MALDI-ToF-Microflex LRF, Brucker Daltonics). An external quadratic multi-point calibration was carried out before each measurement using polyethylene glycol (PEG) mixed in THF with dithranol (DIT). Analysis were performed with DIT as matrix (10 mg/mL) and sodium trifluoroacetic acid (10 mg/mL) as an additive. The polymer (10 mg/mL), the matrix and the additive were mixed in a volumetric ratio of 1/1/0.5 in THF. All the analysis was performed in positive reflectron mode.

Computational Details: The conformational analyses of complexes **2b** and **3b** were carried out by using the Conformer-Rotamer Ensemble Sampling Tool (CREST) based on the GFN-xTB method[18] in which the electronic energies of sampled conformers are estimated with the tight-binding DFT implemented in the xTB software.[19] The most stable conformers were then refined by density functional theory (DFT) in dichloromethane by using the PBE0 functional[20] and def2SVP basis set[21] with Gaussian 16.[22] See Supporting Information for the detailed procedure.

ASSOCIATED CONTENT

Supporting Information

The Supporting Information is available free of charge on the ACS Publications website.

NMR spectra of compounds **L1H-L5H**, **[L2H$_2$][Br], 1a-5a**, **1b-5b**, **2b'** and **4b'**. Variable Temperature NMR spectra of **3b**. DOSY of **2b**, **3b** and **6b**.

Synthesis, characterization and NMR spectra of the FI complexes **6a**, **6b** and **6b'**.
Graph of the PLA M_n values as a function of lactide conversion, Graph of $\ln([M]_0/[M])$ versus time, GPC analysis, MALDI-TOF spectra.
Tables of crystal data for the proligands **L2H-L5H**, **[L2H$_2$][Br],** and for the complexes **2a-5a**, **2b-3b, 4b'**and **6b'**.
Conformational sampling of **2b** and **3b**
Accession Codes
CCDC 2107446, 2107447, 2107448, 2107449, 2107450, 2107451, 2107452, 2107453, 2107454, 2107455, 2107456, 2157220 and 2205595 contain the supporting crystallographic data for this paper for compound **L2H**, **L2H$_2$Br**, **L3H**, **L4H**, **L5H**, **2a**, **3a**, **4a**, **5a**, **2b**, **3b**, **4b'**and **6b'** respectively. These data can be obtained free of charge via www.ccdc.cam.ac.uk/data_request/cif, or by emailing data request@ccdc.cam.ac.uk, or by contacting The Cambridge Crystallographic Data Centre, 12 Union Road, Cambridge CB2 1EZ, UK; fax: +44 1223 336033.

AUTHOR INFORMATION

Corresponding Authors

* E-mail: dagorne@unistra.fr, Tel: +33 (0)3 68 85 15 30;
Raluca.Malacea@u-bourgogne.fr, Tel: +33 (0)3 80 39 90 38;
pierre.le-gendre@u-bourgogne.fr, Tel: +33 (0)3 80 39 60 82;

Notes

The authors declare no competing financial interest.

ACKNOWLEDGMENT

Gaël Stepien, Dr Quentin Bonnin and Marie-José Penouilh are kindly acknowledged for their contribution to DOSY NMR and MALDI-ToF experiments. Prof. Jean-Pierre Couvercelle is warmly thanked for his assistance in GPC measurements. Support was provided by the Ministère de l'Enseignement Supérieur et de la Recherche, and the Centre National de la Recherche Scientifique (CNRS). Conseil Régional de Bourgogne Franche-Comté is acknowledged for financing the PhD grant of B.T. under the "Itinéraire Chercheurs Entrepreneurs" (ICE) program.

REFERENCES

(1) For a review and representative articles about phenoxyimine metal complexes for olefin polymerization and oligomerization, see: (a) Makio, H.; Terao, H.; Iwashita, A.; Fujita, T., FI Catalysts for Olefin Polymerization—A Comprehensive Treatment. *Chem. Rev.* **2011,** *111*, 2363-2449. (b) Wang, C.; Friedrich, S.; Younkin, T. R.; Li, R. T.; Grubbs, R. H.; Bansleben, D. A.; Day, M. W. Neutral Nickel(II)-Based Catalysts for Ethylene Polymerization. *Organometallics* **1998**, *17*, 3149-3151. (c) Younkin, T. R.; Connor, E. F.; Henderson, J. I.; Friedrich, S. K.; Grubbs, R. H.; Bansleben, D. A. Neutral, Single-Component Nickel (II) Polyolefin Catalysts That Tolerate Heteroatoms. *Science* **2000**, *287*, 460-462. (d) Tian, J.; Hustad, P. D.; Coates, G. W. A New Catalyst for Highly Syndiospecific Living Olefin Polymerization: Homopolymers and Block Copolymers from Ethylene and Propylene. *J. Am. Chem. Soc.* **2001**, *123*, 5134-5135. (e) Suzuki, Y.; Kinoshita, S.; Shibahara, A.; Ishii, S.; Kawamura, K.; Inoue, Y.; Fujita, T., Trimerization of Ethylene to 1-Hexene with Titanium Complexes Bearing Phenoxy−Imine Ligands with Pendant Donors Combined with MAO. *Organometallics* **2010,** *29*, 2394-2396. (f) Cai, Z.; Xiao, D.; Do, L. H. Fine-Tuning Nickel Phenoxyimine Olefin Polymerization Catalysts: Performance Boosting by Alkali Cations. *J. Am. Chem. Soc.* **2015**, *137*, 15501-15510. (g) Gao, Y.; Christianson, M. D.; Wang, Y.; Chen, J.; Marshall, S.; Klosin, J.; Lohr, T. L.; Marks, T. J., Unexpected Precatalyst sigma-Ligand Effects in Phenoxyimine Zr-Catalyzed Ethylene/1-Octene Copolymerizations. *J. Am. Chem. Soc.* **2019**, *141*, 7822-7830.
(2) For a review and representative examples of phenoxyimine metal complexes for ROP of cyclic esters, see: (a) Santoro, O.; Zhang, X.; Redshaw, C., Synthesis of Biodegradable Polymers: A Review on the Use of Schiff-Base Metal Complexes as Catalysts for the Ring Opening Polymerization (ROP) of Cyclic Esters. *Catalysts* **2020,** *10*, 800. (b) Nomura, N.; Aoyama, T.; Ishii, R.; Kondo, T. Salicylaldimine−Aluminum Complexes for the Facile and Efficient Ring-Opening Polymerization of ε-Caprolactone. *Macromolecules* **2005**, *38*, 5363-5366. (c) Chen, H.-Y.; Tang, H.-Y.; Lin, C.-C. Ring-Opening Polymerization of Lactides Initiated by Zinc Alkoxides Derived from NNO-Tridentate Ligands. *Macromolecules* **2006**, *39*, 3745-3752. (d) Liu, J.; Iwasa, N.; Nomura, K. Synthesis of Al complexes containing phenoxy-imine ligands and their use as the catalyst precursors for efficient living ring-opening polymerisation of ε-caprolactone. *Dalton Trans.* **2008**, 3978-3988. (e) Pappalardo, D.; Annunziata, L.; Pellecchia, C. Living Ring-Opening Homo- and Copolymerization of ε-Caprolactone and *L*- and *D,L*-Lactides by Dimethyl(salicylaldiminato)aluminum Compounds. *Macromolecules* **2009**, *42*, 6056-6062. (f) García-Valle, F. M.; Tabernero, V.; Cuenca, T.; Mosquera, M. E. G.; Cano, J.; Milione, S. Biodegradable PHB from rac-β-Butyrolactone: Highly Controlled ROP Mediated by a Pentacoordinated Aluminum Complex. *Organometallics* **2018**, *37*, 837-84. (g) McKeown, P.; McCormick, S. N.; Mahon, M. F.; Jones, M. D., Highly active Mg(II) and Zn(II) complexes for the ring opening polymerisation of lactide. *Polym. Chem.* **2018**, *9*, 5339-5347. (h) Payne, J.; McKeown, P.; Mahon, M. F.; Emanuelsson, E. A. C.; Jones, M. D., Mono- and dimeric zinc(II) complexes for PLA production and degradation into methyl lactate – a chemical recycling method. *Polym. Chem.* **2020**, *11*, 2381-2389.
(3) (a) Aratani, T., Catalytic asymmetric synthesis of cyclopropanecarboxylic acids: an application of chiral copper carbenoid reaction. *Pure Appl. Chem.* **1985**, *57*, 1839-1844. (b) Kurono, N.; Ohkuma, T., Catalytic Asymmetric Cyanation Reactions. *ACS Catalysis* **2016**, *6*, 989-1023. (c) Sha, F.; Mitchell, B. S.; Ye, C. Z.; Abelson, C. S.; Reinheimer, E. W.; LeMagueres, P.; Ferrara, J. D.; Takase, M. K.; Johnson, A. R., Catalytic intramolecular hydroamination of aminoallenes using titanium complexes of chiral, tridentate, dianionic imine-diol ligands. *Dalton Trans.* **2019**, *48*, 9603-9616.
(4) (a) Dell'Amico, G.; Marchetti, F.; Floriani, C., Peripheral electrophilic properties of dichloro[*N,N'*-ethylenebis(salicylideneiminato)]titanium(IV): a route leading to a stable Ti–H–B unit. *J. Chem. Soc., Dalton Trans.* **1982**, 2197-2202. (b) Matsui, S.; Mitani, M.; Saito, J.; Tohi, Y.; Makio, H.; Matsukawa, N.; Takagi, Y.; Tsuru, K.; Nitabaru, M.; Nakano, T.; Tanaka, H.; Kashiwa, N.; Fujita, T., A Family of Zirconium Complexes Having Two Phenoxy−Imine Chelate Ligands for Olefin Polymerization. *J. Am. Chem. Soc.* **2001**, *123*, 6847-6856. (c) Normand, M.; Kirillov, E.; Roisnel, T.; Carpentier, J.-F., Meerwein–Ponndorf–Verley-Type Reduction Processes in Aluminum and Indium Isopropoxide Complexes of Imino-Phenolate Ligands. *Organometallics* **2012,** *31*, 5511-5519.
(5) Floriani, C.; Solari, E.; Corazza, F.; Chiesi-Villa, A.; Guastini, C., A trans-Dimethyl Derivative of Octahedral TiIV: Alkylation and Arylation of TiIV-Schiff Base Complexes. *Angew. Chem. Int. Ed.* **1989**, *28*, 64-66.
(6) Chotard, F.; Lapenta, R.; Bolley, A.; Trommenschlager, A.; Balan, C.; Bayardon, J.; Malacea-Kabbara, R.; Bonnin, Q.; Bodio, E.; Cattey, H.; Richard, P.; Milione, S.; Grassi, A.; Dagorne, S.; Le Gendre, P., Phenoxyamidine Zn and Al Complexes: Synthesis, Characterization, and Use in the Ring-Opening Polymerization of Lactide. *Organometallics* **2019**, *38*, 4147-4157.
(7) Nikitin, S. V.; Nikitin, V. V.; Oleynik, I. I.; Oleynik, I. V.; Bagryanskaya, E. G., Activity of phenoxy-imine titanium catalysts in ethylene polymerization: A quantum chemical approach. *J. Mol. Catal. A: Chem.* **2016**, *423*, 285-292.
(8) Kirillov, E.; Roisnel, T.; Carpentier, J.-F., Synthesis and Structural Diversity of Group 4 Metal Complexes with Multidentate Tethered Phenoxy-Amidine and Phenoxy-Amidinate Ligands. *Organometallics* **2012**, *31*, 3228-3240.
(9) Selected examples with Zn and Al complexes, see: (a) Chamberlain, B. M.; Cheng, M.; Moore, D. R.; Ovitt, T. M.; Lobkovsky, E. B.; Coates, G. W., Polymerization of Lactide with Zinc and Magnesium β-Diiminate Complexes: Stereocontrol and Mechanism. *J. Am. Chem. Soc.* **2001**, *123*, 3229-3238. (b) Zhong, Z.; Dijkstra, P. J.; Feijen, J., [(salen)Al]-Mediated, Controlled and Stereoselective Ring-Opening Polymerization of Lactide in Solution and without Solvent: Synthesis of Highly Isotactic Polylactide Stereocopolymers from Racemic d,l-

Lactide. *Angew. Chem. Int. Ed.* **2002**, *41*, 4510-4513. (c) Williams, C. K.; Breyfogle, L. E.; Choi, S. K.; Nam, W.; Young, V. G.; Hillmyer, M. A.; Tolman, W. B., A Highly Active Zinc Catalyst for the Controlled Polymerization of Lactide. *J. Am. Chem. Soc.* **2003,** *125*, 11350-11359. (d) Thevenon, A.; Romain, C.; Bennington, M. S.; White, A. J. P.; Davidson, H. J.; Brooker, S.; Williams, C. K., Dizinc Lactide Polymerization Catalysts: Hyperactivity by Control of Ligand Conformation and Metallic Cooperativity. *Angew. Chem. Int. Ed.* **2016,** *55*, 8680-8685. (e) Chellali, J. E.; Alverson, A. K.; Robinson, J. R. Zinc Aryl/Alkyl β-diketiminates: Balancing Accessibility and Stability for High-Activity Ring-Opening Polymerization of rac-Lactide. *ACS Catalysis* **2022**, 5585-5594.

(10) (a) Schäfer, P. M.; McKeown, P.; Fuchs, M.; Rittinghaus, R. D.; Hermann, A.; Henkel, J.; Seidel, S.; Roitzheim, C.; Ksiazkiewicz, A. N.; Hoffmann, A.; Pich, A.; Jones, M. D.; Herres-Pawlis, S., Tuning a robust system: N,O zinc guanidine catalysts for the ROP of lactide. *Dalton Trans.* **2019,** *48*, 6071-6082. (b) Hermann, A.; Hill, S.; Metz, A.; Heck, J.; Hoffmann, A.; Hartmann, L.; Herres-Pawlis, S., Next Generation of Zinc Bisguanidine Polymerization Catalysts towards Highly Crystalline, Biodegradable Polyesters. *Angew. Chem. Int. Ed.* **2020,** *59*, 21778-21784.

(11) (a) Dunn, P. J., 5.19 - Amidines and N-Substituted Amidines. In *Comprehensive Organic Functional Group Transformations*, Katritzky, A. R.; Meth-Cohn, O.; Rees, C. W., Eds. Elsevier Science: Oxford, 1995; pp 741-782. (b) Dunn, P. J., 5.19 - Amidines and N-Substituted Amidines. In *Comprehensive Organic Functional Group Transformations II*, Katritzky, A. R.; Taylor, R. J. K., Eds. Elsevier: Oxford, 2005; pp 655-699.

(12) (a) Hegarty, A. F.; Chandler, A., Isomerisation about the C–N and C=N bonds of *E*- and *Z*-amidines. *J. Chem. Soc., Chem. Commun.* **1980**, 130-131. (b) aroszewska-Manaj, J.; Oszczapowicz, J.; Makulski, W., Amidines. Part 41.1 Effects of substitution at the amidino carbon atom and at the imino nitrogen atom on the preferred configuration at the C=N bond in the ^{13}C NMR spectra of N^1,N^1-dimethyl-N^2-alkylamidines. *J. Chem. Soc., Perkin Trans. 2* **2001**, 1186-1191. (c) Kalz, K. F.; Hausmann, A.; Dechert, S.; Meyer, S.; John, M.; Meyer, F., Solution Chemistry of N,N'-Disubstituted Amidines: Identification of Isomers and Evidence for Linear Dimer Formation. *Chem. Eur. J.* **2016**, *22*, 18190-18196.

(13) T. Boeré, R.; Klassen, V.; Wolmershäuser, G., Synthesis of some very bulky N,N′-disubstituted amidines and initial studies of their coordination chemistry. *J. Chem. Soc., Dalton Trans.* **1998**, 4147-4154.

(14) Lewiński, J.; Zachara, J.; Starowieyski, K. B.; Ochal, Z.; Justyniak, I.; Kopeć, T.; Stolarzewicz, P.; Dranka, M., Structure Investigations of Group 13 Derivatives of N-Phenylsalicylideneimine. *Organometallics* **2003**, *22*, 3773-3780.

(15) (a) Chisholm, M. H.; Gallucci, J. C.; Zhen, H.; Huffman, J. C., Three-Coordinate Zinc Amide and Phenoxide Complexes Supported by a Bulky Schiff Base Ligand. *Inorg. Chem.* **2001**, *40*, 5051-5054. (b) Darensbourg, D. J.; Choi, W.; Richers, C. P., Ring-Opening Polymerization of Cyclic Monomers by Biocompatible Metal Complexes. Production of Poly(lactide), Polycarbonates, and Their Copolymers. *Macromolecules* **2007**, *40*, 3521-3523. (c) Hung, W.-C.; Huang, Y.; Lin, C.-C., Efficient initiators for the ring-opening polymerization of L-lactide: Synthesis and characterization of NNO-tridentate Schiff-base zinc complexes. *J. Polym. Sci., Part A: Polym. Chem.* **2008**, *46*, 6466-6476. (d) Darensbourg, D. J.; Karroonnirun, O., Ring-Opening Polymerization of Lactides Catalyzed by Natural Amino-Acid Based Zinc Catalysts. *Inorg. Chem.* **2010**, *49*, 2360-2371.

(16) (a) Iwasa, N.; Fujiki, M.; Nomura, K. Ring-opening polymerization of various cyclic esters by Al complex catalysts containing a series of phenoxy-imine ligands: Effect of the imino substituents for the catalytic activity. *J. Mol. Catal. A: Chem.* **2008**, *292*, 67-75. (b) Zhang, W.; Wang, Y.; Sun, W.-H.; Wang, L.; Redshaw, C. Dimethylaluminium aldiminophenolates: synthesis, characterization and ring-opening polymerization behavior towards lactides. *Dalton Trans.* **2012**, *41*, 11587-11596. (c) Normand, M.; Dorcet, V.; Kirillov, E.; Carpentier, J.-F. {Phenoxy-imine}aluminum versus -indium Complexes for the Immortal ROP of Lactide: Different Stereocontrol, Different Mechanisms. *Organometallics* **2013**, *32*, 1694-1709. (d) Chang, M.-C.; Lu, W.-Y.; Chang, H.-Y.; Lai, Y.-C.; Chiang, M. Y.; Chen, H.-Y.; Chen, H.-Y. Comparative Study of Aluminum Complexes Bearing N,O- and N,S-Schiff Base in Ring-Opening Polymerization of ε-Caprolactone and l-Lactide. *Inorg. Chem.* **2015**, *54*, 11292-11298.

(17) Raman, S. K.; Raja, R.; Arnold, P. L.; Davidson, M. G.; Williams, C. K., Waste not, want not: CO_2 (re)cycling into block polymers. *Chem. Commun.* **2019,** *55*, 7315-7318.

(18) Grimme, S.; Bannwarth, C.; Dohm, S.; Hansen, A.; Pisarek, J.; Pracht, P.; Seibert, J.; Neese, F. Fully Automated Quantum-Chemistry-Based Computation of Spin–Spin-Coupled Nuclear Magnetic Resonance Spectra. *Angew. Chem. Int. Ed.* **2017**, *56*, 14763-14769.

(19) Bannwarth, C.; Ehlert, S.; Grimme, S. GFN2-xTB—An Accurate and Broadly Parametrized Self-Consistent Tight-Binding Quantum Chemical Method with Multipole Electrostatics and Density-Dependent Dispersion Contributions. *J. Chem. Theory Comput.* **2019**, *15*, 1652-1671.

(20) Adamo, C.; Barone, V. Toward reliable density functional methods without adjustable parameters: The PBE0 model. *The Journal of Chemical Physics* **1999**, *110*, 6158-6170.

(21) Weigend, F.; Ahlrichs, R. Balanced basis sets of split valence, triple zeta valence and quadruple zeta valence quality for H to Rn: Design and assessment of accuracy. *Phys. Chem. Chem. Phys.*, **2005**, *7*, 3297-3305.

(22) Frisch, M. J.; Trucks, G. W.; Schlegel, H. B.; Scuseria, G. E.; Robb, M. A.; Cheeseman, J. R.; Scalmani, G.; Barone, V.; Petersson, G. A.; Nakatsuji, H.; Li, X.; Caricato, M.; Marenich, A. V.; Bloino, J.; Janesko, B. G.; Gomperts, R.; Mennucci, B.; Hratchian, H. P.; Ortiz, J. V.; Izmaylov, A. F.; Sonnenberg, J. L.; Williams; Ding, F.; Lipparini, F.; Egidi, F.; Goings, J.; Peng, B.; Petrone, A.; Henderson, T.; Ranasinghe, D.; Zakrzewski, V. G.; Gao, J.; Rega, N.; Zheng, G.; Liang, W.; Hada, M.; Ehara, M.; Toyota, K.; Fukuda, R.; Hasegawa, J.; Ishida, M.; Nakajima, T.; Honda, Y.; Kitao, O.; Nakai, H.; Vreven, T.; Throssell, K.; Montgomery Jr., J. A.; Peralta, J. E.; Ogliaro, F.; Bearpark, M. J.; Heyd, J. J.; Brothers, E. N.; Kudin, K. N.; Staroverov, V. N.; Keith, T. A.; Kobayashi, R.; Normand, J.; Raghavachari, K.; Rendell, A. P.; Burant, J. C.; Iyengar, S. S.; Tomasi, J.; Cossi, M.; Millam, J. M.; Klene, M.; Adamo, C.; Cammi, R.; Ochterski, J. W.; Martin, R. L.; Morokuma, K.; Farkas, O.; Foresman, J. B.; Fox, D. J.: Gaussian 16 Rev. C.01. Wallingford, CT, 2016.